Statistical Properties of Scale-Invariant Helical Magnetic Fields and Applications to Cosmology

Axel Brandenburg[a,b,c,d,e] **Ruth Durrer**[f] **Tina Kahniashvili**[c,g,h] **Sayan Mandal**[1c] **Weichen Winston Yin**[i,c]

[a]Laboratory for Atmospheric and Space Physics, University of Colorado, Boulder, CO 80303, USA

[b]JILA and Department of Astrophysical and Planetary Sciences, University of Colorado, Boulder, CO 80303, USA

[c]McWilliams Center for Cosmology and Department of Physics, Carnegie Mellon University, 5000 Forbes Ave, Pittsburgh, PA 15213, USA

[d]Nordita, KTH Royal Institute of Technology and Stockholm University, Roslagstullsbacken 23, 10691 Stockholm, Sweden

[e]Department of Astronomy, AlbaNova University Center, Stockholm University, 10691 Stockholm, Sweden

[f]Département de Physique Théorique and Center for Astroparticle Physics, Université de Geneve, Quai E. Ansermet 24, 1211 Genéve 4, Switzerland

[g]Department of Physics, Laurentian University, Ramsey Lake Road, Sudbury, ON P3E 2C, Canada

[h]Abastumani Astrophysical Observatory, Ilia State University, 3-5 Cholokashvili St., 0194 Tbilisi, Georgia

[i]Department of Physics, University of California Berkeley, Berkeley, CA 94720

E-mail: sayanm@cmu.edu

Abstract. We investigate the statistical properties of isotropic, stochastic, Gaussian distributed, helical magnetic fields characterized by different shapes of the energy spectra at large length scales and study the associated realizability condition. We discuss smoothed magnetic fields that are commonly used when the primordial magnetic field is constrained by observational data. We are particularly interested in scale-invariant magnetic fields that can be generated during the inflationary stage by quantum fluctuations. We determine the correlation length of such magnetic fields and relate it to the infrared cutoff of perturbations produced during inflation. We show that this scale determines the observational signatures of the inflationary magnetic fields on the cosmic microwave background. At smaller scales, the scale-invariant spectrum changes with time. It becomes a steeper weak-turbulence spectrum at progressively larger scales. We show numerically that the critical length scale where this happens is the turbulent-diffusive scale, which increases with the square root of time.

---

[1]Corresponding author: Authors are listed alphabetically

Contents

1 Introduction

The origin of cosmic magnetic fields is one of the big open questions in astrophysics and space physics [1–3]. It is generally thought that these magnetic fields are the result of the amplification of weak initial seed fields. It is also clear now that μG-strength magnetic fields were already present in spiral galaxies (like our Milky Way) when the universe was about a third of its present age [4–6]. This poses strong constraints on the initial seed magnetic field strength and its amplification timescale. There are two basic magnetogenesis scenarios currently under discussion: a bottom-up (astrophysical) scenario, where the seed is typically very weak and magnetic fields are transferred from local sources within galaxies to larger scales [7], and a top-down (primordial) scenario where a significant seed field is generated prior to galaxy formation in the early universe on scales that are now large [8]. The primordial magnetogenesis scenario is supported by recent observations suggesting that lower bounds of the order of 10^{-18} to 10^{-19} G exist for the intergalactic magnetic fields[1], (see refs. [9–18], also ref. [19] for discussions on possible uncertainties in the measurements of blazar spectra). In addition to these lower limits from observations, there exist also *upper* limits of the order of a few nG for the intergalactic magnetic field [2, 3].

A cosmological magnetic field contributes to the radiation-like energy density, and sources all three helicities of linear gravitational perturbations [20][2] which lead to corresponding temperature and

---

[1]Initially, the 10^{-15}–10^{-16} G limit had been obtained [9, 10] based on studying blazar TeV photons which produce a cascade flux in the GeV band after absorption by the extragalactic background light (EBL). Considering the expected cascade flux with the assumption of a constant TeV flux gives this estimate. These bounds have been subsequently reconsidered after accounting for the fact that the source observation period (of the order of a few years) limits the flux activity in the TeV blazars [16]. The simultaneous observations of blazars in the GeV and TeV bands lead to weaker limits of the order of 10^{-18}–10^{-19} G [12, 16].

[2]These are (i) the scalar mode – density perturbations, (ii) the vector mode – vorticity perturbations, and (iii) the tensor mode – gravitational waves, that do not have an analogy within Newtonian physics, while Newtonian physics admits the analogy for density (and vorticity) perturbations as magnetosonic (and Alfvén) waves.

polarization anisotropies of the cosmic microwave background (CMB). In addition it induces Faraday rotation of the CMB polarization direction, and affects large-scale structure (LSS) formation; see ref. [3] and references therein. All these effects can be used to constrain the magnetic field strength, and as we show below, the magnetogenesis scenarios. Upper limits for cosmological magnetic fields can also be obtained through CMB constraints on Faraday rotation [21], and these limits are independent of those from magnetic helicity [22–24]. In addition, upper limits on extragalactic magnetic fields can be derived from Faraday rotation measurements of polarized emission of distant quasars [25–28]. Other tests leading to *upper* limits on large-scale correlated magnetic fields are based on their effects on big bang nucleosynthesis (BBN) [29], the CMB (including CMB fluctuations, polarization, distortions, non-gaussianity, etc, see ref. [30] and references therein), or LSS formation (for a recent review, see [3]). The lower limit on the intergalactic magnetic field in voids, of the order of 10^{-18} G on 1 Mpc scales, is a relatively recent constraint in modern astrophysics (see ref. [31]), and could very well be the result of the amplification of a primordial cosmological field [15].

One of several plausible mechanisms for the origin of these cosmic magnetic fields is to assume that a seed magnetic field has been generated in the early universe [3]. Below we discuss two basic possibilities for primordial magnetogenesis – inflation and cosmological phase-transitions. The purpose of this paper is to discuss magnetic energy and helicity spectra produced by these mechanisms and to investigate relevant length scales, which is no longer straightforward in inflationary magnetogenesis.

Inflationary Magnetogenesis: Magnetogenesis can occur during inflation by the amplification of quantum vacuum fluctuations, as was shown in several pioneering works [32, 33]. The rapid exponential growth and the induced stretching of the field during inflation can produce a very large correlation length of the observed magnetic fields today. In addition, inflation also provides a natural way to generate modes from quantum fluctuations of the field inside the Hubble radius, which are subsequently converted into classical fluctuations as they exit the Hubble horizon. Such fields can have a scale-invariant (or a nearly scale-invariant) spectrum. These, among several other properties, make inflationary magnetogenesis an attractive scenario (see [3] for a recent review).

The Maxwell action describing the electromagnetic field is conformally invariant, and the Friedmann-Lemaître-Robertson-Walker (FLRW) metric describing the evolution of the universe is conformally flat. Therefore, the process leading to quantum excitation of the magnetic field must break conformal invariance. For this, one has to introduce couplings of the electromagnetic field that break conformal invariance. There are several possibilities to achieve this. These include coupling of the field to the inflaton, or to the curvature (the Riemann tensor). Several authors [8, 32–64] have explored a range of models dealing with inflationary magnetogenesis. The inflation-generated magnetic field scenarios should be considered with some caution due to the possibility of a "strong coupling problem" and significant backreaction [65–70], which is not a problem for the phenomenological, effective classical model, see ref. [71], for Lorentz-violating magnetogenesis [72], or if the function that couples the inflaton to the electromagnetic field has sharp and non-monotonic features [73, 74].

Phase Transition Magnetogenesis: Some magnetogenesis mechanisms make use of the symmetry breaking during cosmological phase transitions (e.g. electroweak or QCD) [75–101]. If the magnetic field originated during a cosmological phase transitions, its spectrum is constrained by the causality requirement [102], in particular the magnetic field correlation length must be less than or equal to the Hubble length scale at the moment of generation.

Usually, a first-order phase transition is needed for magnetic fields of substantial strength and correlation scales to arise, the idea being that bubbles of the new phase start nucleating in the space filled with the old phase; these bubbles then expand and collide with each other, ultimately filling the entire space with the new phase. Such processes are highly out of equilibrium (and violent), and can generate significant turbulence, amplifying the fields [103]. In this scenario, the correlation length of the magnetic field (i.e., the magnetic domain length scale) can be associated with the phase transition bubble size [104]. One can also associate processes like baryogenesis with these phase transitions [88].

There are two phase transitions of interest in the early universe – the electroweak phase transition occurring at a temperature of $T \sim 100$ GeV, and the QCD phase transition occurring at $T \sim 150$ MeV [1–3, 105]. However, these transitions are usually (i.e., within the standard model of particle physics) not of first-order, but are simple *crossovers*, so the transition occurs smoothly [106–108]. There has

been much research about the conditions or extensions of the standard model under which these transitions become first-order (possibilities include having a large leptonic chemical potential for the QCD transition [109], supersymmetric extensions for electroweak phase transitions [110], etc).

One of the most important properties of the primordial magnetic fields is their helicity. Magnetogenesis mechanisms that involve a parity violation can lead to magnetic fields with non-zero helicity (see for example refs. [42, 46, 61, 62, 72, 78, 79, 82, 88, 90, 94–96, 111–114]). It is a well known fact that magnetic helicity is an important factor defining the evolution of turbulent magnetic fields in the early universe. In particular, helicity conservation sets constraints on the decay of magnetic fields in the early universe leading to an inverse cascade of energy in the helical fields. Thus, helicity leads to magnetic fields with a larger correlation length that decay slower compared with non-helical fields [115–117]. However, in the case of nearly scale-invariant magnetic fields, the correlation length is almost frozen in [118].

The mean magnetic energy and helicity densities are related by the realizability condition – one of the topics of the present study (see section 3). The realizability condition limits the maximal helicity that random magnetic fields can sustain [119]. Hence, magnetic fields with a lower value of helicity can be defined as states with fractional helicity. On the other hand, numerical simulations show that magnetic fields with zero helicity can still undergo a slower non-helical inverse transfer of magnetic fields [2, 120].

We study the evolution of magnetic fields in the expanding universe by solving the magneto-hydrodynamic (MHD) evolution equations for these fields and the fluid density and velocity. These equations describe the coupling between random magnetic fields and turbulent motions, as well as amplification and damping. To account for the expansion of the universe, these equations are rewritten in terms of comoving quantities [121], The numerical simulations are done using the PENCIL CODE (https://github.com/pencil-code) [122], which is a high order finite-difference code for solving equations involving compressible magnetohydrodynamic flows.

As mentioned above, we study the statistical properties of random helical magnetic fields generated during the early universe, with special emphasis on the realizability conditions and its cosmological applications. In section 2, we review in some detail the spectral and statistical properties of magnetic fields, taking special care to relate the average quantities and the various characteristic length scales to the magnetic field spectra, and define the smoothed magnitudes of the magnetic field and the helicity, that are widely used when analyzing observational data. In section 3, we discuss the realizability condition for generic magnetic fields, and relate it to the smoothed magnitudes. In section 3.1, we consider two different types of shape for the energy spectrum, and formulate a method to make the realizability condition hold consistently at all scales also for inflationary, nearly scale-invariant fields. In section 4, we present the results of numerical simulations, such as the evolution of the magnetic mean energy density, the correlation length, and the fractional helicity, which grows owing to magnetic energy decay.

One of the major points of the present paper is the study of cosmological applications. In section 5 we discuss cosmological magnetic field amplitudes and helicity limits obtained from CMB and LSS data. Readers familiar with MHD might want to skip over sections 2 and 3 since much of what we present there can be found in books.

In this paper, we propose to extend the results from the Planck satellite [30], taking into account the magnetohydrodynamic evolution of the primordial plasma until the epoch of reionization. To the best of our knowledge, such an analysis has not been done before. This is important since fields with partial initial helicity become fully helical at a later stage in their evolution [124]. Furthermore there is some confusion in the literature regarding the dependence of scalar quantities like the total magnetic energy density and the rms density on helicity. This arises from the fact that the expression for, e.g., the spectrum of the magnetic energy density—a fourth order correlation function in the magnetic field—includes the helicity power spectrum. We have explicitly shown that, after integration, the helicity drops out and does not contribute to the energy density power spectrum. This has not previously been demonstrated, it seems. Similar integrals involving the Lorentz force, for example, can still remain finite, however. Further investigation is needed, which is beyond the scope of this paper. We show that the best way to constrain the helicity is to use parity odd CMB spectra like

C_ℓ^{TB} or C_ℓ^{EB}, [125, 126] that are zero if there is no magnetic helicity (and/or other parity violating other sources). We revisit the current upper limits of ref. [30] on the magnetic field, accounting for the magnetic field coupling with the primordial plasma, and consequently MHD turbulence evolution from the moment of generation until the recombination epoch. We also obtain the upper bounds on maximal inflationary, nearly scale-invariant magnetic helicity accounting for magnetic field evolution [118] and the combined upper limits on the magnetic field strength (through CMB and LSS data) [127]. In section 6, we present some concluding remarks.

Throughout the paper, we set $\hbar = c = k_B = 1$, and we use the Lorentz-Heaviside units to express magnetic fields, such that the magnetic energy density is $\rho_M(\mathbf{x}) = \mathbf{B}^2(\mathbf{x})/2$. Unless otherwise specified, we imply a summation over repeated indices, and Latin indices run through $1, \ldots, 3$.

2 Modeling a helical magnetic field

Seed magnetic fields are generated in the early universe (see ref. [3] for a review of possible primordial magnetogenesis scenarios) from either random quantum fluctuations during inflation, or from a first order phase transition, which proceeds via bubble nucleation, a violent and stochastic process. It is not surprising, therefore, that the generated magnetic fields are themselves random and stochastic. As already mentioned, the considerations presented in this section are not new, but in order to eliminate recent confusions in the literature, we want to lay them out carefully and clearly.

To define correlation functions or power spectra, we take an ensemble average, i.e., an average over many realizations. We assume that the generated magnetic field is statistically homogeneous and isotropic and that it obeys Gaussian statistics.

2.1 Magnetic field spectrum

All statistical information of a stochastically homogeneous and isotropic Gaussian magnetic field can be obtained through its two-point correlation function, $\mathcal{B}_{ij}(\mathbf{r}) \equiv \langle B_i(\mathbf{x})B_j(\mathbf{x} + \mathbf{r})\rangle$ [128], which, in its most general form, can be written as

$$\mathcal{B}_{ij}(\mathbf{r}) = M_N(r)\delta_{ij} + \left[M_L(r) - M_N(r)\right]\hat{r}_i\hat{r}_j + M_H(r)\epsilon_{ijl}r_l, \tag{2.1}$$

where $\langle\cdots\rangle$ denotes the average over the statistical ensemble and $\hat{r}_i = r_i/|\mathbf{r}|$. In this case, it is equivalent to the volume average over all $\mathbf{x}$ due to homogeneity. The functions $M_N(r)$, $M_L(r)$, and $M_H(r)$ are the *lateral* (normal, N), *longitudinal* (L), and *helical* (antisymmetric, H) components of the magnetic field correlation function, respectively. Due to isotropy, all components depend only on $r \equiv |\mathbf{r}|$ (as there is no a preferred direction, $\langle\mathbf{B}(\mathbf{x})\rangle = 0$, for a stochastic magnetic field). Since ε_{ijk} is invariant under rotation, the rotational symmetry is preserved also for antisymmetric helical fields.

Although $\mathcal{B}_{ij}(\mathbf{r})$ is rotationally invariant, the presence of the antisymmetric part ($\propto \varepsilon_{ijl}r_l M_H(r)$) means that parity (mirror) symmetry is violated. It is easy to see that

$$\mathcal{B}_{ij}(\mathbf{r}) = \mathcal{B}_{ji}(-\mathbf{r}). \tag{2.2}$$

The contribution of the helical part to each diagonal term $\mathcal{B}_{ii}$ (no summation here) of the magnetic field two-point correlation function vanishes. Thus, the diagonal terms, and hence the trace, *do not* contain any information on the asymmetric part. This statement is true for both solenoidal (divergence-free) and irrotational (curl-free) fields.

The normal, $M_N(r)$, longitudinal, $M_L(r)$, and helical, $M_H(r)$ components of the magnetic correlation function are obtained from the correlation function $\mathcal{B}_{ji}$ via the following projection operations:

$$P_{ij}(\hat{\mathbf{r}})\mathcal{B}_{ij}(\mathbf{r}) = 2M_N(r), \tag{2.3}$$

$$\hat{r}_i\hat{r}_j\mathcal{B}_{ij}(\mathbf{r}) = M_L(r), \tag{2.4}$$

$$\varepsilon_{ijm}\hat{r}_m\mathcal{B}_{ij}(\mathbf{r}) = 2rM_H(r), \tag{2.5}$$

where $P_{ij}(\hat{\mathbf{r}}) = \delta_{ij} - \hat{r}_i\hat{r}_j$ is the projector tensor into the plane normal to $\mathbf{r}$. Indeed, the trace, given by $\mathcal{B}_{ii}(\mathbf{r}) = \delta_{ij}\mathcal{B}_{ij}(\mathbf{r}) = 2M_N(r) + M_L(r)$, is independent of the antisymmetric part.

Since the magnetic field is divergence-free, $\nabla \cdot \mathbf{B} = 0$, M_{L} and M_{N} are not independent but related by

$$M_{\mathrm{N}}(r) = \frac{1}{2r}\frac{d}{dr}\left[r^2 M_{\mathrm{L}}(r)\right] = M_{\mathrm{L}}(r) + \frac{r}{2}\frac{d}{dr}M_{\mathrm{L}}(r). \tag{2.6}$$

Hence, there are only two independent functions $M_{\mathrm{L}}(r)$ and $M_{\mathrm{H}}(r)$ that determine the full magnetic two-point correlation function. Requiring that the magnetic field has a well defined power spectrum also for $k \to 0$, we have

$$\int d^3\mathbf{r}\,|\mathcal{B}_{ii}(\mathbf{r})| < \infty. \tag{2.7}$$

As we will show below, this inequality also ensures that the average (mean) magnetic energy density $\mathcal{E}_{\mathrm{M}} = \langle \mathbf{B}(\mathbf{x}) \cdot \mathbf{B}(\mathbf{x}) \rangle/2$ is well defined in wavenumber space $\mathbf{k}$.

Let us now consider the spectral (Fourier) decomposition of our stochastic magnetic field amplitudes[3] $\mathbf{B}(\mathbf{k})$. Reality of $\mathbf{B}(\mathbf{x})$ implies $\mathbf{B}(\mathbf{k}) = \mathbf{B}^{\star}(-\mathbf{k})$, and due to statistical homogeneity the 2-point statistical average is of the form

$$\langle B_i^{\star}(\mathbf{k})B_j(\mathbf{k}') \rangle = (2\pi)^3\delta^{(3)}(\mathbf{k}-\mathbf{k}')\mathcal{F}_{ij}^{(B)}(\mathbf{k}), \tag{2.9}$$

where $\langle \cdots \rangle$ again denotes ensemble average, but now in wavenumber space. The matrix $\mathcal{F}_{ij}^{(B)}(\mathbf{k})$ is called the three-dimensional (3D) power spectrum of the magnetic field, and in fact, it is the Fourier transform of the magnetic field two-point correlation function $\mathcal{B}_{ij}(\mathbf{r})$ (see appendix A):

$$\mathcal{B}_{ij}(\mathbf{r}) = \frac{1}{(2\pi)^3}\int d^3\mathbf{k}\,e^{-i\mathbf{k}\cdot\mathbf{r}}\mathcal{F}_{ij}^{(B)}(\mathbf{k}), \tag{2.10}$$

$$\mathcal{F}_{ij}^{(B)}(\mathbf{k}) = \int d^3\mathbf{r}\,e^{i\mathbf{k}\cdot\mathbf{r}}\mathcal{B}_{ij}(\mathbf{r}). \tag{2.11}$$

Translational invariance of the magnetic field is reflected in the presence of the Dirac delta function $\delta^{(3)}(\mathbf{k}-\mathbf{k}')$ on the right hand side of equation (2.9). For the general case, when the isotropic stochastic Gaussian magnetic field has non-zero helicity ($M_{\mathrm{H}}(r) \neq 0$), the 3D spectrum matrix components $\mathcal{F}_{ij}^{(B)}(\mathbf{k})$ satisfy the following reality conditions:

$$\mathcal{F}_{ij}^{(B)}(\mathbf{k}) = \mathcal{F}_{ji}^{(B)}(-\mathbf{k}) = [\mathcal{F}_{ij}^{(B)}]^{\star}(-\mathbf{k}) = [\mathcal{F}_{ji}^{(B)}]^{\star}(\mathbf{k}). \tag{2.12}$$

Defining $P_{ij}(\hat{\mathbf{k}}) = \delta_{ij} - \hat{k}_i\hat{k}_j$, the projection operator onto the plane normal to $\mathbf{k}$ with $\hat{k}_i = k_i/k$, $k = |\mathbf{k}|$, the divergence-free condition of the magnetic field requests the following form for $\mathcal{F}_{ij}(\mathbf{k})$

$$\frac{\mathcal{F}_{ij}^{(B)}(\mathbf{k})}{(2\pi)^3} = P_{ij}(\hat{\mathbf{k}})\frac{E_{\mathrm{M}}(k)}{4\pi k^2} + i\varepsilon_{ijl}k_l\frac{H_{\mathrm{M}}(k)}{8\pi k^2}. \tag{2.13}$$

The most general form for the function $\mathcal{F}_{ij}(\mathbf{k})$ is

$$\mathcal{F}_{ij}(\mathbf{k}) = P_{ij}(\hat{\mathbf{k}})\mathcal{F}_{\mathrm{N}}(k) + \hat{k}_i\hat{k}_j\mathcal{F}_{\mathrm{L}}(k) + i\varepsilon_{ijl}k_l\mathcal{F}_{\mathrm{H}}(k). \tag{2.14}$$

The functions $\mathcal{F}_{\mathrm{N}}(k)$, $\mathcal{F}_{\mathrm{L}}(k)$, and $\mathcal{F}_{\mathrm{H}}(k)$ represent the normal, longitudinal, and helical (antisymmetric) parts of the magnetic 3D spectrum, and they are integrals over the corresponding function in real space [4] Using integrals given in Eqs. 2.15, as well as the spherical Bessel function identity

---

[3]We define the Fourier transform of the magnetic field, $\mathbf{B}(\mathbf{x})$, with the following normalization:

$$\mathbf{B}(\mathbf{k}) = \int d^3\mathbf{x}\,e^{i\mathbf{k}\cdot\mathbf{x}}\mathbf{B}(\mathbf{x}), \qquad \mathbf{B}(\mathbf{x}) = \frac{1}{(2\pi)^3}\int d^3\mathbf{k}\,e^{-i\mathbf{k}\cdot\mathbf{x}}\mathbf{B}(\mathbf{k}). \tag{2.8}$$

[4] The functions $\mathcal{F}_{\mathrm{N}}(k)$, $\mathcal{F}_{\mathrm{L}}(k)$, and $\mathcal{F}_{\mathrm{H}}(k)$ can be expressed in terms of M_{N}, M_{L}, and M_{H} as

$$\mathcal{F}_{\mathrm{L}}(k) = 4\pi\int_0^{\infty} dr\,r^2\left[j_0(kr)M_{\mathrm{L}} + \frac{2j_1(kr)}{kr}(M_{\mathrm{N}} - M_{\mathrm{L}})\right],$$

$$\mathcal{F}_{\mathrm{N}}(k) = 4\pi\int_0^{\infty} dr\,r^2\left[j_0(kr)M_{\mathrm{N}} + \frac{j_1(kr)}{kr}(M_{\mathrm{L}} - M_{\mathrm{N}})\right],$$

$$\mathcal{F}_{\mathrm{H}}(k) = -8\pi\int_0^{\infty} dr\,r^2\left[\frac{j_1(kr)}{kr}M_{\mathrm{H}}\right], \tag{2.15}$$

$(x^2 j_1(x))' = x^2 j_0$, one sees immediately that (2.6) implies $\mathcal{F}_{\mathrm{L}}(k) \equiv 0$ for a divergence-free field. The function $E_{\mathrm{M}}(k)$ is determined by the symmetric part of the magnetic field 3D spectrum, it is usually referred to as the spectral energy density, $\int dk\, E_{\mathrm{M}}(k) = \mathcal{E}_{\mathrm{M}}$, see section 2.2, below, and it can be expressed in terms of the Fourier transform of the normal component of the correlation function given in equation (2.1), $\mathcal{F}_{\mathrm{N}}(k)$ as $E_{\mathrm{M}}(k) = \mathcal{F}_{\mathrm{N}}(k)/(4\pi k^2)$. The function $H_{\mathrm{M}}(k)$ is the antisymmetric part of the 3D magnetic field spectrum, usually referred to as the spectral density of the magnetic helicity, $\int dk H_{\mathrm{M}}(k) = \mathcal{H}_{\mathrm{M}}$, see section 2.4 below. It can be expressed in terms of the helical component of the Fourier transform of the correlation function equation (2.1), $H_{\mathrm{M}}(k) = \mathcal{F}_{\mathrm{H}}(k)/(2\pi k)$. The magnetic field spectral energy and helicity densities are typically given by simple power laws in a certain wavenumber range; generally different spectral ranges are characterized by different spectral indices,

$$E_{\mathrm{M}}(k) \propto k^{n_E}, \quad H_{\mathrm{M}}(k) \propto k^{n_{\mathrm{H}}}. \tag{2.16}$$

Of particular interest are the spectral shapes at large length scales, i.e., small wavenumbers, and, from now on, whenever unspecified, "spectral index" refers to the spectral index at the large-scale asymptotics. These spectral indices n_E and n_{H} determine the shapes of spectral energy and helicity of the magnetic field *only* at large length scales (small wavenumbers). They are defined by $\lim_{k \to 0} E_{\mathrm{M}}/k^{n_E} = \text{finite}$ and $\lim_{k \to 0} H_{\mathrm{M}}/k^{n_{\mathrm{H}}} = \text{finite}$.

2.2 Mean and rms energy densities

The mean magnetic energy density per unit volume, $\mathcal{E}_{\mathrm{M}}$, is given by

$$\mathcal{E}_{\mathrm{M}} = \langle \rho_{\mathrm{M}}(\mathbf{x}) \rangle = \frac{1}{2}\langle |\mathbf{B}(\mathbf{x})|^2 \rangle = \frac{1}{2}\mathcal{B}_{ii}(0) = M_{\mathrm{N}}(0) + \frac{1}{2}M_{\mathrm{L}}(0). \tag{2.17}$$

Since $M_{\mathrm{N}}(0) = M_{\mathrm{L}}(0)$,[5] we have

$$M_{\mathrm{N}}(0) = M_{\mathrm{L}}(0) = \frac{2}{3}\mathcal{E}_{\mathrm{M}}. \tag{2.18}$$

Note again that the mean energy is independent of the helicity given by $M_{\mathrm{H}}(r)$ or $\mathcal{F}_{\mathrm{H}}(k)$. The quantity $\mathcal{B}_{ii}(0)$ is given by the trace of the 3D spectrum, $\mathcal{F}_{ii}(\mathbf{k})$ (which is continuous at $\mathbf{k} \to 0$, provided the magnetic energy density does not diverge at infinity), and thus $\mathcal{B}_{ii}(0) = \delta_{ij} \lim_{\mathbf{r} \to 0} \mathcal{B}_{ij}(\mathbf{r})$. We have

$$\mathcal{E}_{\mathrm{M}} = \frac{1}{2(2\pi)^3}\delta_{ij} \lim_{\mathbf{r} \to 0} \int d^3\mathbf{k}\, e^{-i\mathbf{k}\cdot\mathbf{r}} \mathcal{F}_{ij}^{(B)}(\mathbf{k}) = \int dk\, E_{\mathrm{M}}(k). \tag{2.19}$$

Thus $E_{\mathrm{M}}(k)$ describes the distribution of the magnetic energy density in wavenumber space, which justifies its definition as the *spectral energy density of the magnetic field*.[6] The requirement that the magnetic energy density converges toward infinity ($k \to 0$) implies that $n_E > -1$. A spectrum with $n_E \to -1$, i.e., $E(k) \propto k^{-1}$ is a *scale-invariant* spectrum. Such a magnetic field can be generated during the inflationary epoch; for a review see [3] and references therein.

We denote the integral $\int_0^\infty dk\, E_{\mathrm{M}}(k)$ by $\int dk\, E_{\mathrm{M}}(k)$. In reality, the power law (with different spectral shapes in the different regimes) for $E_{\mathrm{M}}(k)$ only holds below the magnetic field cutoff scale k_D, i.e. $E_{\mathrm{M}}(k) \to 0$ for $k > k_D$.[7]

---

where $j_n(x)$ is the spherical Bessel function of order n. The divergenceless condition of the magnetic field implies $k_i \mathcal{F}_{ij}(\mathbf{k}) = k_j \mathcal{F}_{ij}(\mathbf{k}) = 0$, and thus the longitudinal component $\mathcal{F}_{\mathrm{L}}(k)$ must be vanishing for the divergence-free field.

[5]The equality can be shown as follows. We rotate the coordinate frame $\mathbf{x} \to \mathbf{x}'$, so that the axis $\mathbf{e}_1$ is now in the direction of $\mathbf{r}$. Then there will only be two independent components of the matrix $\mathcal{B}'_{ij}(\mathbf{r}')$. These components correspond to the normal and longitudinal components, and they must be equal to each other at $\mathbf{r} = 0$. This is also obtained from (2.6), assuming $M'_L(r)|_{r=0} < \infty$. See [128] for details.

[6] The symmetric spectra $M_{\mathrm{N}}(r)$ and $M_{\mathrm{L}}(r)$ in terms of $E_{\mathrm{M}}(k)$ and the spherical Bessel functions $j_n(x)$ can be written as:

$$M_{\mathrm{L}}(r) = 2\int_0^\infty dk E_{\mathrm{M}}(k)\frac{j_1(kr)}{kr}, \qquad M_{\mathrm{N}}(r) = \int_0^\infty dk\left[j_0(kr) - \frac{j_1(kr)}{kr}\right]E_{\mathrm{M}}(k). \tag{2.20}$$

These are just the inverse Fourier transforms of the expressions in footnote 4 for the case $\mathcal{F}_{\mathrm{L}} = 0$.

[7]More precisely for $k > k_D$ the magnetic field spectral energy density experiences the exponential cutoff, $E_{\mathrm{M}}(k) \propto e^{-(k/k_D)^2}$ for $k > k_D$.

The magnetic root mean square (rms) energy density is defined as

$$\mathcal{E}_{\mathrm{M}}^{\mathrm{rms}} = \left[\langle |\rho_{\mathrm{M}}(\mathbf{x})|^2 \rangle \right]^{1/2} = \frac{1}{2} \sqrt{\langle |\mathbf{B}(\mathbf{x})|^4 \rangle}. \tag{2.21}$$

Hence,

$$\mathcal{E}_{\mathrm{M}}^{\mathrm{rms}} = \frac{1}{2} \lim_{\mathbf{r} \to 0} \sqrt{\mathcal{B}_{ii,jj}(\mathbf{r})}, \tag{2.22}$$

where $\mathcal{B}_{ij,lm}$ is the four-point correlation function of the magnetic field, defined as

$$\mathcal{B}_{ij,lm}(\mathbf{r}) = \langle B_i(\mathbf{x}) B_j(\mathbf{x}) B_l(\mathbf{x}+\mathbf{r}) B_m(\mathbf{x}+\mathbf{r}) \rangle. \tag{2.23}$$

As we consider a Gaussian magnetic field, we can apply Wick's theorem and express the four-point correlation function in terms of the two-point correlation functions,

$$\mathcal{B}_{ij,lm}(\mathbf{r}) = \mathcal{B}_{ij}(0)\mathcal{B}_{lm}(0) + \mathcal{B}_{il}(\mathbf{r})\mathcal{B}_{jm}(\mathbf{r}) + \mathcal{B}_{im}(\mathbf{r})\mathcal{B}_{jl}(\mathbf{r}). \tag{2.24}$$

We emphasize that the first term on the rhs of equation (2.24) is usually discarded (see, for example, ref. [129]) because it cannot be obtained through **k**-space considerations.

From the definition of the 4-point function it is clear that,

$$\mathcal{B}_{ij,lm}(\mathbf{r}) = \mathcal{B}_{lm,ij}(\mathbf{r}) = \mathcal{B}_{ji,lm}(\mathbf{r}) = \mathcal{B}_{ij,ml}(\mathbf{r}). \tag{2.25}$$

We now calculate the trace of (2.23) and obtain,

$$\mathcal{B}_{ii,ll}(\mathbf{r}) = 9M_{\mathrm{N}}^2(0) + 4M_{\mathrm{N}}^2(r) + 2M_{\mathrm{L}}^2(r) + 4r^2 M_{\mathrm{H}}^2(r). \tag{2.26}$$

Reconstructing equation (2.26) from the magnetic field rms energy density power spectrum must be done with caution: the first constant term $9M_{\mathrm{N}}^2(0)$ will be missing when naively taking the direct Fourier transform of $\mathcal{B}_{ii,ll}(k)$. To find the rms magnetic energy density, we now take the limit of $\mathcal{B}_{ii,ll}(\mathbf{r})$ as $\mathbf{r} \to 0$. Equation (2.22) then gives (see appendix B)

$$\mathcal{E}_{\mathrm{M}}^{\mathrm{rms}} = \frac{1}{2}\sqrt{15}M_{\mathrm{N}}(0) = \sqrt{\frac{5}{3}}\mathcal{E}_{\mathrm{M}}. \tag{2.27}$$

We conclude that *the rms magnetic energy density* $\mathcal{E}_{\mathrm{M}}^{\mathrm{rms}}$, *just like the average magnetic energy density* $\bar{\rho}_{\mathrm{M}} = \mathcal{E}_{\mathrm{M}}$, *does not depend on magnetic helicity.*[8] For this it is important that we define the helical component as $\epsilon_{ijl} r^l M_H(r)$ so that it vanishes as $\mathbf{r} \to 0$, which it must as a consequence of its antisymmetry under parity.

2.3 Characteristic length scales

In this section we define the relevant characteristic length scales for the magnetic fields that are related to the correlation and damping length scales. We distinguish between statistically relevant length scales and smoothing length scales: Statistical length scales are determined fully by the magnetic field configuration and the properties of the plasma (viscosity, diffusivity, etc), while smoothing length scales are introduced for convenient interpretation and *normalization* purposes. In cosmology, it is often convenient to use a smoothing length of 1 Mpc since an amplitude of about 10^{-9} Gauss on this scale is required to form the observed magnetic fields in clusters by pure contraction, without a dynamo mechanism [130, 131]. Depending on the magnetic field generation mechanism, this scale of 1 Mpc can be substantially larger than the magnetic correlation length (e.g., for magnetic fields generated during the electroweak phase transition), while for other mechanisms, 1 Mpc can be a small fraction of the magnetic correlation length (e.g., for inflationary magnetic fields). We discuss the normalization aspects in section 2.5.

---

[8]Note that ref. [129] gives a potentially misleading expression in their equation (3.4), implying the presence of a helical contribution to the rms energy density. That expression is only the $\mathcal{O}(k^0)$ term of the fuller expressions given in their Appendix B, and could be misunderstood. The bottom left panel of their figure 1 indicates positive and negative contributions from small and large k, suggesting vanishing rms energy density, although it is not explicitly mentioned.
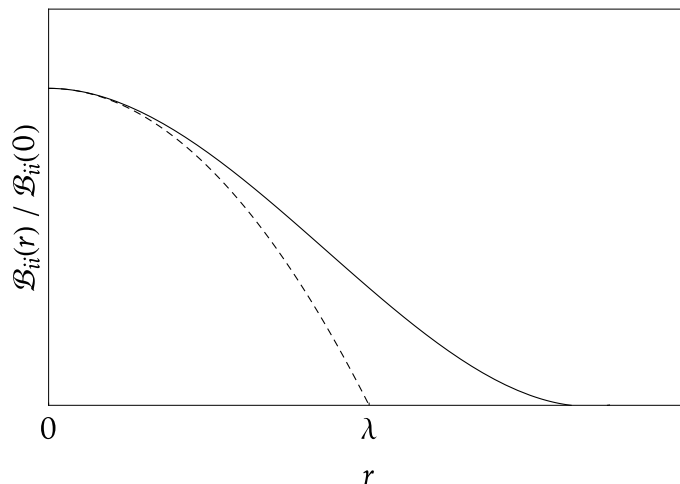
Figure 1. The damping scale is the length segment that is cut off on the abscissa by a parabola that can be locally fit to the $B_{ii}(r)$ curve at its apex ($r = 0$), see also ref. [128].

Let us first consider the characteristic length scales that are constructed solely from integration of the spectral magnetic energy. The magnetic integral scale is defined as [128]

$$\xi_{\mathrm{M}}(t) = k_{\mathrm{M}}^{-1} = \frac{\int_0^\infty dk\, k^{-1} E_{\mathrm{M}}(k, t)}{\mathcal{E}_{\mathrm{M}}(t)}. \tag{2.28}$$

There are various possibilities to construct additional length scales from the second derivative of the magnetic two-point correlation function. In particular, we define the *differential* scale for the magnetic field as [128]

$$\lambda_{\mathrm{M}} = \left| \frac{\mathcal{B}_{ii}(0)}{\mathcal{B}_{ii}''(0)} \right|^{1/2}. \tag{2.29}$$

The differential length scale characterizes the scale beyond which correlations between two points are significantly washed out. In figure 1 we illustrate the meaning of the differential length scale. The wavenumber corresponding to the differential length scale λ_{M} is known as the magnetic *Taylor* microscale wavenumber,

$$k_{\mathrm{MT}}^2 = \frac{\int_0^\infty dk\, k^2 E_{\mathrm{M}}(k)}{\mathcal{E}_{\mathrm{M}}} \tag{2.30}$$

with $\lambda_{\mathrm{M}} = k_{\mathrm{MT}}^{-1}$. In Kolmogorov's hydrodynamic turbulence theory, dissipation is described through the mean kinetic energy dissipation per unit mass: $\epsilon_{\mathrm{K}} = 2\nu \int dk\, k^2 \tilde{E}_{\mathrm{K}}(k)$, where ν is the kinematic viscosity, and the tilde on E (and later also on $\mathcal{E}$) is used here and below to indicate energies or spectral energies per unit mass, applying normalization by $p + \rho$, where p and ρ denote the pressure and the energy density of the plasma. Thus, analogously to ϵ_{K}, the magnetic energy dissipation is given by $\epsilon_{\mathrm{M}} \propto 2\eta \int dk\, k^2 \tilde{E}_{\mathrm{M}}(k)$. The magnetic dissipation wavenumber is defined through

$$k_{\mathrm{MD}}^4 = \frac{\epsilon_{\mathrm{M}}}{\eta^3} = \frac{2 \int_0^\infty dk\, k^2 \tilde{E}_{\mathrm{M}}(k)}{\eta^2}, \tag{2.31}$$

where η is the magnetic diffusivity. In the present case, however, the turbulent flow is driven entirely by the magnetic field and the magnetic energy spectrum follows a weak turbulence (WT) spectrum of the form

$$\tilde{E}_{\mathrm{M}}(k) = C_{\mathrm{WT}} \left(\epsilon_{\mathrm{M}} v_{\mathrm{A}} k_{\mathrm{M}} \right)^{1/2} k^{-2}, \tag{2.32}$$

where $C_{\mathrm{WT}} \approx 1.9$ is a Kolmogorov-type constant for magnetically dominated turbulence [117], and $v_{\mathrm{A}} = (2\tilde{\mathcal{E}}_{\mathrm{M}})^{1/2}$ is the Alfvén speed. Defining now a k-dependent Lundquist number as $\mathrm{Lu}(k) = v_{\mathrm{A}}(k)/\eta k$ with $v_{\mathrm{A}}^2(k) = 2kE_{\mathrm{M}}(k)$ and defining a WT dissipation wavenumber through $\mathrm{Lu}(k_{\mathrm{WT}}) = 1$, we find[9]

$$k_{\mathrm{WT}}^6 = (2C_{\mathrm{WT}})^2 \, \mathrm{Lu} \, k_{\mathrm{M}}^2 \, k_{\mathrm{MD}}^4. \tag{2.33}$$

In section 5 below, we show the values of some of the characteristic length scales during the MHD decay.

2.4   Current and magnetic helicity

The antisymmetric part of the magnetic field spectrum, $M_{\mathrm{H}}(r)$, is related to the magnetic helicity. It is also related to the current helicity, but this is usually less crucial than the magnetic helicity, which satisfies a conservation equation. The mean magnetic helicity density over a volume V is defined as

$$\mathcal{H}_{\mathrm{M}} = \lim_{V \to \infty} \frac{1}{V} \int_V d^3\mathbf{x} \, \mathbf{A} \cdot \mathbf{B} = \lim_{V \to \infty} \frac{1}{V} \int_V d^3\mathbf{x} \left(\mathrm{curl}^{-1}\mathbf{B} \right) \cdot \mathbf{B} \, . \tag{2.34}$$

In the mathematical literature, this is called a *generalized asymptotic form of the Hopf invariant* [132], or the *measure of line linkage* of the $\mathbf{B}$ field. This quantity cannot be defined locally, and in a realistic situation the infinite volume should be understood as a 3D volume where the magnetic field is determined.

Note that the form of $\mathcal{H}_{\mathrm{M}}$ is gauge-dependent, unless the domain is periodic [133] or the normal component of $\mathbf{B}$ vanishes at infinity [134]. However, this only affects the magnetic helicity spectrum at the largest scales [135]. Let us also note that in hydrodynamics, the kinetic helicity of the velocity field $\mathbf{v}$ is

$$\mathcal{H}_K = \frac{1}{V} \int_V d^3\mathbf{x} \left[\mathbf{v} \cdot (\nabla \times \mathbf{v}) \right]. \tag{2.35}$$

By analogy, it is customary to define the current helicity of the magnetic field $\mathbf{B}$ as

$$\mathcal{H}_C = \frac{1}{V} \int_V d^3\mathbf{x} \left[\mathbf{B} \cdot (\nabla \times \mathbf{B}) \right], \tag{2.36}$$

which is gauge-invariant.

Replacing $\frac{1}{V} \int d^3\mathbf{x}$ by an ensemble average, $\langle \cdots \rangle$, and using the definition of $H_{\mathrm{M}}(k)$ in equation (2.13), we find that the magnetic helicity can be written as

$$\mathcal{H}_{\mathrm{M}} = \int dk \, H_{\mathrm{M}}(k) \, , \tag{2.37}$$

while the current helicity can be expressed as

$$\mathcal{H}_C = \int dk \, k^2 H_{\mathrm{M}}(k) \, . \tag{2.38}$$

2.5   Smoothed magnetic field and helicity

We also define the smoothed magnetic field amplitude and magnetic helicity density over a smoothing length scale $\sim \lambda$ using a Gaussian window function $e^{-\lambda^2 k^2}$,

$$B_\lambda^2 = \int E_{\mathrm{M}}(k) \, e^{-\lambda^2 k^2} \, dk, \quad H_\lambda = \int H_{\mathrm{M}}(k) \, e^{-\lambda^2 k^2} \, dk, \tag{2.39}$$

which can be related to the average energy by eliminating the normalization. This gives rise to

$$\frac{B_\lambda^2}{\mathcal{E}_{\mathrm{M}}} = \frac{\displaystyle\int E_{\mathrm{M}}(k) \, e^{-\lambda^2 k^2} \, dk}{\displaystyle\int E_{\mathrm{M}}(k) \, dk} \, , \quad \frac{H_\lambda}{\mathcal{H}_{\mathrm{M}}} = \frac{\displaystyle\int H_{\mathrm{M}}(k) \, e^{-\lambda^2 k^2} \, dk}{\displaystyle\int H_{\mathrm{M}}(k) \, dk} \, . \tag{2.40}$$

---

[9] Inserting $k = k_{\mathrm{WT}}$ into $\mathrm{Lu}(k_{\mathrm{WT}}) = 1$, we have $1 = (\eta k_{\mathrm{WT}})^{-1} \sqrt{2k_{\mathrm{WT}} C_{\mathrm{WT}} \, (\epsilon_{\mathrm{M}} v_{\mathrm{A}} k_{\mathrm{M}})^{1/2} \, k_{\mathrm{WT}}^{-2}}$. Raising this to the fourth power and solving for k_{WT} yields $k_{\mathrm{WT}}^6 = (2\,C_{\mathrm{WT}})^2 \epsilon_{\mathrm{M}} v_{\mathrm{A}} k_{\mathrm{M}}/\eta^4$. The combination $\epsilon_{\mathrm{M}}/\eta^3$ is just k_{MD}^4 from equation equation (2.31) and $\mathrm{Lu} \equiv v_{\mathrm{A}}/\eta k_{\mathrm{M}}$ is now defined as a k-independent Lundquist number.

3   The realizability condition

If the magnetic diffusivity is very small, as it is for the highly conductive plasma of the early universe, it can be shown that the *magnetic helicity is conserved*. This leads to the theorem [136]

> *The eigenfield of* curl^{-1} *corresponding to the eigenvalue L of the largest modulus*
> *has minimum energy in the class of divergence free fields obtained from*   (3.1)
> *the eigenfield under the action of volume-preserving diffeomorphisms.*

In other words, if L_- and L_+ denote the smallest and largest eigenvalues of the curl^{-1} operator respectively, with $L_- < 0 < L_+$, then for every divergence-free field $\mathbf{B}$, we have

$$L_-|\mathbf{B}(\mathbf{x})|^2 \leq \left(\mathrm{curl}^{-1}\mathbf{B}\right)\cdot\mathbf{B} \leq L_+|\mathbf{B}(\mathbf{x})|^2, \tag{3.2}$$

which implies

$$\left|\frac{\left(\mathrm{curl}^{-1}\mathbf{B}\right)\cdot\mathbf{B}}{L}\right| \leq |\mathbf{B}(\mathbf{x})|^2. \tag{3.3}$$

Here $L = \max\{-L_-, L_+\}$ is the larger of the moduli of the two eigenvalues. Taking an ensemble average leads to

$$\left\langle|\mathbf{B}(\mathbf{x})|^2\right\rangle = 2\mathcal{E}_\mathrm{M} \geq \left|\frac{\left\langle\left(\mathrm{curl}^{-1}\mathbf{B}\right)\cdot\mathbf{B}\right\rangle}{L}\right| = \left|\frac{\mathcal{H}_\mathrm{M}}{L}\right|. \tag{3.4}$$

For a field with eigenvalue $\pm L$, the equality sign holds but in general we have $|\mathcal{H}_\mathrm{M}| \leq 2|L|\mathcal{E}_M$.

It is justified to assume that $|L|$ is of the order of the magnetic integral length scale, $|L| \lesssim \xi_\mathrm{M}$, since this is the maximal length scale that can be associated with the size of a domain. This leads to the well-known realizability condition

$$|\mathcal{H}_\mathrm{M}| \leq 2\xi_M\mathcal{E}_\mathrm{M}. \tag{3.5}$$

This equation, together with the definitions in equations (2.19), (2.28) and (2.40), leads to

$$|H_\lambda| \leq f(\lambda)B_\lambda^2, \tag{3.6}$$

where

$$f(\lambda) = 2\left|\frac{\int H_\mathrm{M}(k)\,e^{-\lambda^2 k^2}\,dk}{\int H_\mathrm{M}(k)\,dk}\right| \bigg/ \frac{\int E_\mathrm{M}(k)\,e^{-\lambda^2 k^2}\,dk}{\int k^{-1}E_\mathrm{M}(k)\,dk}\,. \tag{3.7}$$

In the examples discussed below, which are all for the fully helical case with $kH_\mathrm{M} = 2E_\mathrm{M}$, we show that for $\lambda \ll \xi_\mathrm{M}$, we have $f(\lambda) \simeq \xi_\mathrm{M}$, while for $\lambda \gg \xi_\mathrm{M}$, we have $f(\lambda) \simeq \lambda$. This is simply because in the Batchelor subinertial range, we have $H_\mathrm{M}(k) \propto k^3$, while $E_\mathrm{M}(k) \propto k^4$ (see section 3.2 below), so $H_\lambda \propto \lambda^{-4}$ and $B_\lambda^2 \equiv E_\lambda \propto \lambda^{-5}$.

3.1   Normalized magnetic field and helicity

To satisfy the condition (3.6) on all scales, we need to ensure that the realizability condition embodied by equation (3.7) holds on all scales. For this purpose we analyze magnetic fields with different spectral energy distributions employing statistical properties of random fields from the theory of turbulence. In this approach, we split the stochastic field into its large-scale and small-scale spectra in wavenumber space. We define the large-scale spectrum at wavenumbers smaller than the integral scale of the random field $k < k_1 = \xi_\mathrm{M}^{-1}$. By comparison, the small-scale spectrum, corresponding to the inertial range of turbulence, occurs at $k > k_1$. We proceed with detailed calculations for two relevant cases.
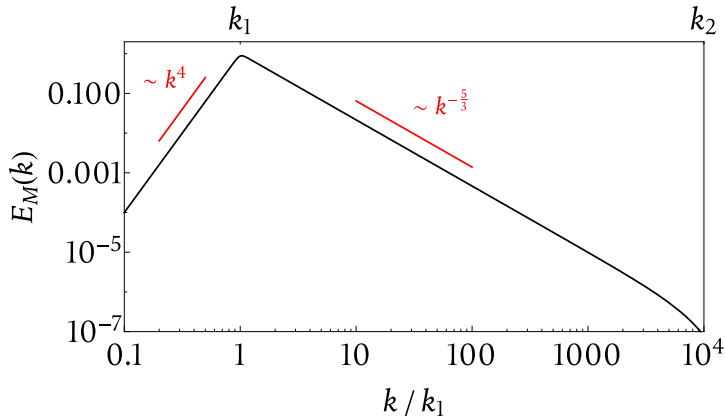
Figure 2. The spectral distribution of the energy of random magnetic fields matching the Batchelor spectrum at large scales ($k < k_1$) and Kolmogorov spectrum at small scales ($k > k_1$) in arbitrary units. The dissipative cutoff occurs at $k > k_2$.

3.2 Batchelor spectrum

The large-scale part of the spectrum of the turbulent fluctuations is often described by a Batchelor spectrum. In this case the energy spectrum at large scales grows as $\sim k^4$. This behavior at large scales is a consequence of causality [102]: If the correlation function in real space has finite support, and since correlations have been generated in the finite past and can spread out no faster than with the speed of light, its Fourier transform, $\mathcal{F}_{ij}(\mathbf{k})$, must be analytic. The nonanalytic prefactor $P_{ij}(\hat{\mathbf{k}})$ then requires that $\mathcal{F}_{\mathrm{N}} \propto k^2$ and hence $E_{\mathrm{M}} \propto k^4$. On scales where the spectrum has already been affected by turbulence, i.e., above the integral wavenumber (in the following referred to as k_1), the spectral energy decreases according to the classical Kolmogorov exponent $k^{-5/3}$, often described as the inertial range of turbulence. At length scales smaller than some dissipative length scale (with corresponding wavenumber defined as k_2) the spectral energy undergoes an exponential cutoff. The spectral distribution of the energy of random magnetic field can be modeled as

$$E_{\mathrm{M}}(k) \propto \frac{k^4 \, \exp[-(k/k_2)^2]}{\left[1 + (k/k_1)^{(5/3+4)q}\right]^{1/q}} \; , \tag{3.8}$$

and $H_{\mathrm{M}}(k) = 2k^{-1}E_{\mathrm{M}}(k)$. We use $q = 5$ to make the transition between the two subranges sufficiently sharp, see figure 2. Note that the correlation length ξ_{M} for such a spectral shape is *finite*. The function $f(\lambda)$ is plotted in figure 3.

Expanding the field in terms of the polarization basis, on can write the magnetic energy spectrum as the sum of two positive definite contributions and the magnetic helicity spectrum is then related to the difference of these two contributions [102, 137]. This leads directly to the realizability condition in wavenumber space,

$$|H_{\mathrm{M}}(k)| \leq 2k^{-1}E_{\mathrm{M}}(k) \, . \tag{3.9}$$

Note that a maximally helical magnetic field for which this inequality becomes an equality, is either in a purely positive or in a purely negative helicity configuration.

There is a special case when the integral scale of the random field matches the spectral cutoff wavenumber $k_1 = k_2$. In this case, the initial increase of the spectral energy at large scales is followed by an exponential cutoff at the integral scale, where the energy reaches a maximum. Hence, no turbulence occurs past the integral scale and a laminar regime dominates. Such a situation can
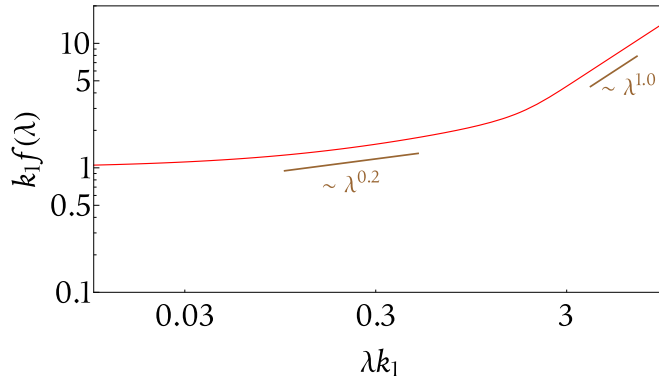
Figure 3. The function $f(\lambda)$ defined in (3.7), for a Batchelor spectrum at large scales. We assume a maximally helical field where the inequality (3.9) is saturated. For $\lambda k_1 \ll 1$, we have $f(\lambda) \to k_1^{-1}$, while for $\lambda k_1 > 1$, $f(\lambda) \sim \lambda$. For intermediate values, $\lambda k_1 \approx 0.3$, we find $f(\lambda) \sim \lambda^{0.2}$.

be realized at very low Reynolds number, which is not relevant to cosmology. For cosmological applications the inertial range of the spectrum, where spectral energy decays with wavenumber in $k_1 < k < k_2$ is an important component contributing to the general form of the random magnetic field configuration.

3.3 Scale-invariant spectrum

A scale-invariant spectrum has $E(k) \sim k^{n_E}$, with $n_E \to -1$ for $k_0 < k < k_1$. For length scales smaller than $\sim k_1^{-1}$, turbulence is fully developed and the spectrum may be a Kolmogorov spectrum proportional to $k^{-5/3}$ or a WT spectrum proportional to k^{-2}, as given by equation (2.32). However if $n_E = -1$ at very large scales, the correlation length is unbounded and the integral proportional to $\int dk\, k^{-1} E(k)$ does not converge. We therefore cannot use equation (3.9) directly. To deal with this situation, we have to modify the spectrum at very large scales for $k < k_0$. In the inflationary case we may consider this to be the horizon scale at the beginning of inflation [118]. We assume the spectrum to have a k^4 dependence at $k < k_0$, a k^{-1} intermediate range for $k_0 < k < k_1$, a $k^{-5/3}$ inertial range for $k_1 < k < k_2$, and an exponential cut-off for $k > k_2$. We can model it as (see figure 4)

$$E_{\mathrm{M}}(k) \propto \frac{k^{-1} \exp[-(k/k_2)^2]}{\left[1 + (k/k_0)^{-(4+1)q} + (k/k_1)^{-(\tilde{n}_{\mathrm{E}}+1)q}\right]^{1/q}}, \tag{3.10}$$

where we choose again, $q = 5$. We consider the fully helical case, $H_{\mathrm{M}}(k) = 2k^{-1} E_{\mathrm{M}}(k)$, and $\tilde{n}_{\mathrm{E}}$ is chosen to be either $-5/3$ or -2. Owing to the Batchelor subinertial range for $k < k_0$, the correlation length is always finite, and we can use equation (3.9) for $k \to 0$. The function $f(\lambda)$ is plotted in figure 6 for different values of k_1/k_0 between 1 and 10^4, comparing two values for the spectral inertial range exponent $\tilde{n}_{\mathrm{E}}$ of -2 and $-5/3$. The difference between these cases with different $\tilde{n}_{\mathrm{E}}$ is significant only for $k_0\lambda \ll 1$ and if k_1/k_0 small. For large values of k_1/k_0, there is now a clear $\lambda^{1/3}$ subrange for $0.1 < k_0\lambda < 1$. As shown in the inset of figure 6, this slope emerges non-trivially from both E_λ and H_λ being non-power laws.

Inflation-generated magnetic fields have a large integral scale, because it becomes exponentially amplified by a factor of $\sim e^{60}$. Turbulence develops and gradually leads to a $k^{-5/3}$ or k^{-2} spectrum, followed by an exponential cutoff at a damping wavenumber k_{MD} or k_{WT}.
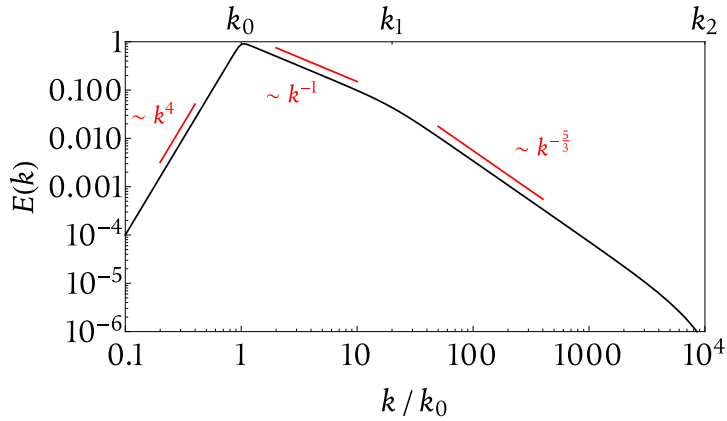
Figure 4. The scale-invariant spectrum, with a k^4 dependence at low k. We have chosen $k_1 = 20k_0$.
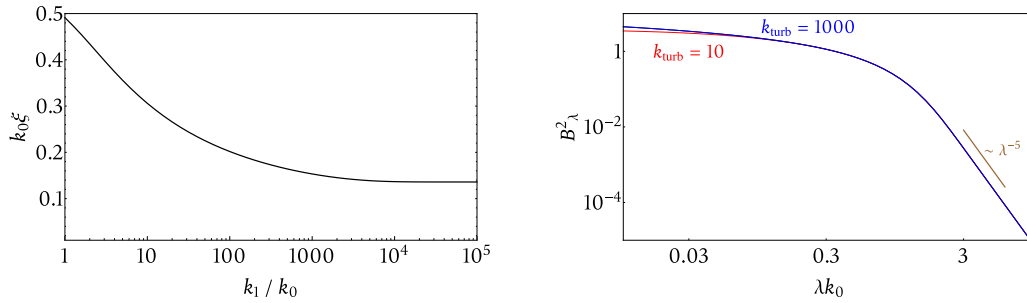

Figure 5. Left: We show $k_0\xi_{\mathrm{M}}(k_1)$, as a function of k_1/k_0. Right: B_λ^2 for $k_{\mathrm{turb}}/k_0 \equiv k_1/k_0 = 10$ (red) and 1000 (blue).

The dependence of the smoothed magnetic field on the smoothing scale λ is shown in the right panel of figure 5.

4   Numerical simulations

Our considerations above have not addressed the time evolution of the magnetic energy spectrum. This is the purpose of the present section. To see how the spectrum changes with time, we solve the
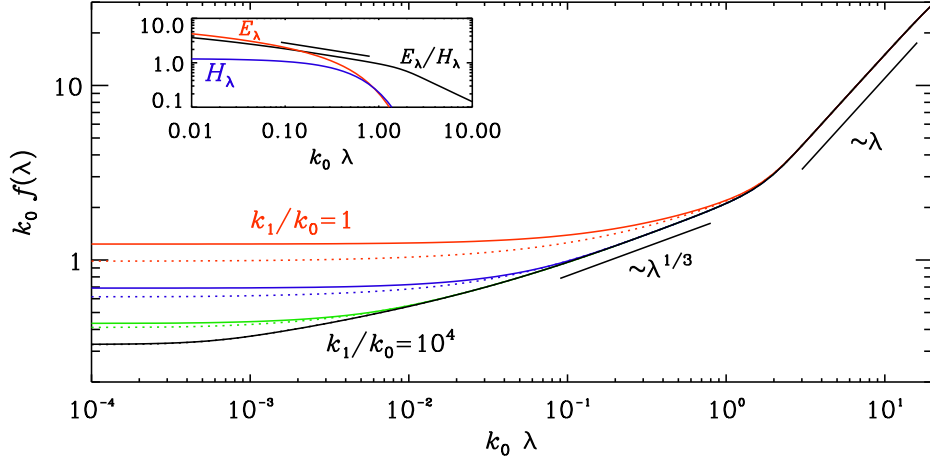
Figure 6. The function $f(\lambda)$ for a scale-invariant spectral subrange between k_0 and k_1, followed by a turbulent inertial range with either $\tilde{n}_{\rm E} = -2$ (solid lines) or $\tilde{n}_{\rm E} = -5/3$ (dotted lines) for $k_1/k_0 = 1$ (red), 10 (blue), 10^2 (green), and 10^4 (black). The inset shows that the 1/3 slope emerges non-trivially from both E_λ and H_λ being non-power laws.
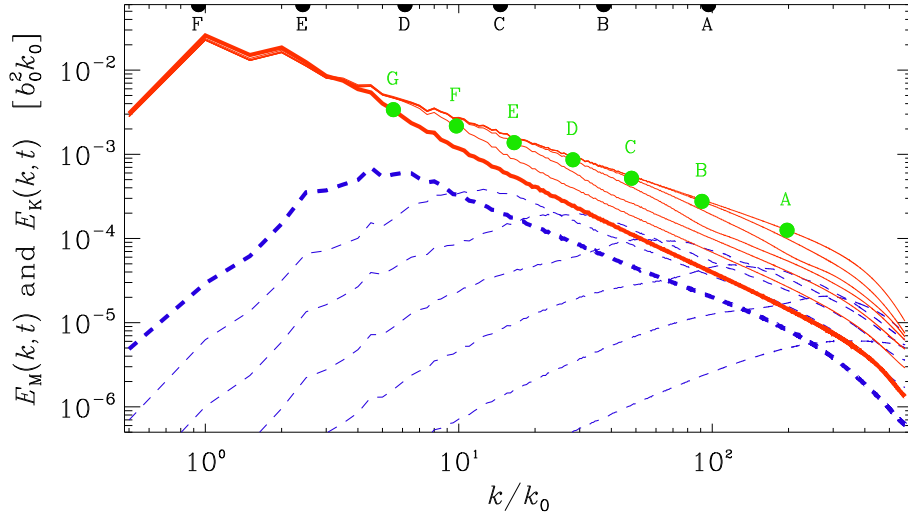
Figure 7. Magnetic (red) and kinetic (blue) energy spectra at early times after having initialized the magnetic field with a spectrum of the form equation (3.10). The green symbols on the red lines denote the position of $k_\star(t)$, as given in equation (4.4), while the black symbols on the upper abscissa denote the location of the horizon wavenumber $k_{\rm hor}(t)$. The times for spectra indicated by the letters A–G are $ck_0t = 0.05, 0.13, 0.34, 0.8, 2.1, 5.3,$ and 15 respectively.

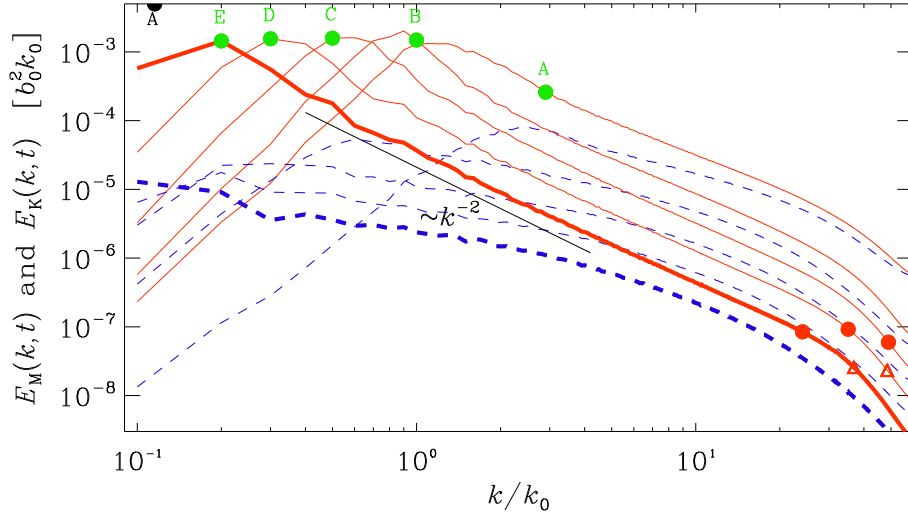hydromagnetic equations for an isothermal relativistic gas with pressure $p = \rho/3$ [118, 121]

$$\frac{\partial \ln \rho}{\partial t} = -\frac{4}{3}\left(\boldsymbol{\nabla} \cdot \mathbf{u} + \mathbf{u} \cdot \boldsymbol{\nabla} \ln \rho\right) + \frac{1}{\rho}\left[\mathbf{u} \cdot (\mathbf{J} \times \mathbf{B}) + \eta \mathbf{J}^2\right], \tag{4.1}$$

$$\frac{\partial \mathbf{u}}{\partial t} = -\mathbf{u} \cdot \boldsymbol{\nabla}\mathbf{u} + \frac{\mathbf{u}}{3}\left(\boldsymbol{\nabla} \cdot \mathbf{u} + \mathbf{u} \cdot \boldsymbol{\nabla} \ln \rho\right) - \frac{\mathbf{u}}{\rho}\left[\mathbf{u} \cdot (\mathbf{J} \times \mathbf{B}) + \eta \mathbf{J}^2\right]$$
$$-\frac{1}{4}\boldsymbol{\nabla} \ln \rho + \frac{3}{4\rho}\mathbf{J} \times \mathbf{B} + \frac{2}{\rho}\boldsymbol{\nabla} \cdot (\rho\nu\mathbf{S}), \tag{4.2}$$

$$\frac{\partial \mathbf{B}}{\partial t} = \nabla \times (\mathbf{u} \times \mathbf{B} - \eta\mathbf{J}), \tag{4.3}$$

– 14 –

Figure 8. Similar to figure 7, but for $k_0/k_{\min} = 10$ and 1152^3 meshpoints resolution. The times are indicated by the letters A–E for $ck_0 t = 9$, 70, 270, 900, and 2500. The red triangles and red filled symbols on the respective magnetic energy spectra denote the positions of k_{MD} and k_{WT}, respectively, provided they fall inside the plot range. Note that k_{WT} is significantly smaller than k_{MD}, for which all earlier times are still outside the plot range.

where $\mathsf{S}_{ij} = \frac{1}{2}(u_{i,j} + u_{j,i}) - \frac{1}{3}\delta_{ij}\boldsymbol{\nabla}\cdot\mathbf{u}$ is the rate-of-strain tensor, ν is the viscosity, and η is the magnetic diffusivity. We consider a periodic domain with sidewalls L and volume L^3, so the smallest wavenumber is $k_{\min} = 2\pi/L$.

In ref. [118], we have already considered the case with an initial k^{-1} spectrum that extends all the way to $k = k_{\min}$, i.e., with no k^4 subinertial range for small k. However, as discussed above, somewhere beyond the event horizon, the spectrum must effectively have a k^4 subrange. To resolve the full wavenumber range, we consider a numerical resolution of 2304^3 mesh points, restricting ourselves to early times only. We clearly see that at early times the spectrum does not change at small wavenumbers. As time goes on, smaller and smaller values of k are affected by the growing velocity field. In figure 7 we show the temporal evolution of the value of k where the spectrum begins to depart from the initial k^{-1} spectrum. We see that this growth is well described by a turbulent-diffusive growth like

$$k_\star(t) \approx \xi_M(t)\,(\eta_{\rm turb} t)^{-1/2} \approx (u_{\rm rms} k_M t/3)^{-1/2}, \tag{4.4}$$

where $\eta_{\rm turb} \approx u_{\rm rms}/3k_M$ is an approximation to the *turbulent* magnetic diffusivity [138]. The ratio $3\eta_{\rm turb}/\eta$ is the magnetic Reynolds number, which has values of around $20{,}000$ in Run A and 500 in Run B. The values of $k_\star(t)$, indicated by green dots, agree well with the positions where the spectrum departs from the initial k^{-1} subrange. Note also that the horizon wavenumber $k_{\rm hor}(t) = (ct)^{-1}$ is always smaller than $k_\star(t)$. Note that the k^4 subinertial range begins to appear within the horizon for $ck_0 t > 5$, corresponding to symbol F in figure 7.

The late time evolution is shown in figure 8, where we see that soon k_M drops well below the initial value k_0. This indicates the begin of the regular inverse cascade of magnetic helicity. The speed at which ξ_M increases is then governed by the usual helicity evolution with $\xi_M \propto t^q$, as can easily be derived from dimensional arguments.

5 Applications in cosmology

The Planck collaboration has recently published a comprehensive study deriving upper limits for a primordial magnetic field based on the measurements of CMB anisotropies and polarization; see

ref. [30]. They used the value of the magnetic field smoothed over 1 Mpc to define upper bounds on the magnetic energy density and the magnetic helicity density; see their equations (2) and (13).

The smoothed fields used in [30] are simply related to the ones defined in section 2.5[10] via $B_\lambda^2 = 2\bar{B}_\lambda^2$ and $\bar{\mathcal{B}}_\lambda^2 = \mathcal{H}_C$ In ref. [30] the magnetic field spectrum is supposed to have a fixed spectral shape in all regions with $k < k_2 = k_D =$ the damping scale. They neglect the presence of a turbulent regime for $k_I = k_1 < k < k_D$ and characterize the symmetric magnetic power spectrum by $E_M(k) \propto k^{n_E}$ and the antisymmetric spectrum by $H_M(k) \propto k^{n_H}$. As we have shown above, such a description assumes that $k_I \equiv k_D$ where k_D is determined through the Alfvén wave damping scale and is related to the amplitude of the magnetic field; see equation (3) of ref. [30]. For a stochastic magnetic field that has a fixed spectral slope up to the damping scale, $E_M(k) \propto k^{n_E}$ for $k \leq k_D$, the Alfvén wave damping wavenumber depends on the rms magnetic field, $B_{\rm rms} \equiv \sqrt{2\mathcal{E}_M}$ and the spectral index n_E as [139], and is given by

$$\frac{k_D}{1 \text{ Mpc}^{-1}} = 1.4 \sqrt{\frac{(2\pi)^{n_E+1}h}{\Gamma\left(\frac{n_E+3}{2}\right)}} \left(\frac{10^{-7} \text{ Gauss}}{B_{\rm rms}}\right), \tag{5.2}$$

where h is the Hubble constant in units of 100 km s^{-1} Mpc^{-1}.

As we have described above, we determine the magnetic damping scale as a scale where the magnetic energy spectrum decays exponentially, and the magnetic field power (in the short-wave length scales) is negligible when compared to the long-wave length or inertial regimes. In figure 8, we indicate the positions of $k_{\rm MD}$ and $k_{\rm WT}$. In all cases, they are indeed much larger that the values of k_M and are therefore only important on very small length scales.

More importantly, the magnetic field is evolving from the moment of generation until recombination when the CMB photons decouple: this evolution can be described as free decay in MHD turbulence, which leads to a growth of the magnetic field correlation length and the decay of the magnetic field amplitude, see section 4 and [120] for the decay laws. Here we assume that the magnetic field has been generated with its maximal *comoving* strength of order of 10^{-6} Gauss. This limit comes from BBN data, which limits the number or relativistic species present at $T = T_{\rm BBN} \sim 0.1$MeV. Since a magnetic field scales like a relativistic species, we can translate this to a magnetic field amplitude, which is 10^{-6} Gauss (comoving).

Magnetic fields generated at the electroweak cosmological phase transition are well below the current bounds (which are of the order of 10^{-9}Gauss) at recombination, and thus these fields *will not leave any observable traces on the CMB* unless a mechanism that will significantly alter the magnetic field evolution via MHD which is discussed here (that seems to be unlikely).

The situation is somewhat more optimistic for magnetic fields generated during the QCD phase transition since the correlation length is larger. But again, the amplitude and correlation scales of the obtained fields are far too small to leave a detectable imprint on the CMB which requires $B_\lambda \gtrsim 10^{-9}$Gauss.

The bounds on the spectral index as obtained by the Planck collaboration was due to their assumption of a flat prior distribution of the PMF. It has been shown that such a bound vanishes when logarithmic priors are used [140]. This shows that a 'blind trust' in Markov Chain Monte Carlo (MCMC) results is problematic and that the result depends on the choice of the prior. It is probably fair to say that for a positive definite quantity, A, a flat prior in $\log(A)$ is more appropriate than a flat prior in A.

In order to constrain the magnetic helicity, we need to observe parity odd CMB spectra (such as EB) since the parity-even spectra (such as EE, BB, or cross correlations) depend on both the symmetric and the helical parts [125, 126, 129, 134]. In other words, we need a measurement that depends solely on the helical component in order to break the degeneracy between $E_M(k)$ and $H_M(k)$. This cannot be provided by scalar quantities like the mean or rms energy densities, since it is shown that

---

[10]In their convention,

$$\bar{B}_\lambda^2 = \int_0^\infty \frac{dk \, k^2}{2\pi^2} e^{-k^2\lambda^2} \mathcal{F}_M(k), \quad \bar{\mathcal{B}}_\lambda^2 = \lambda \int_0^\infty \frac{dk \, k^3}{4\pi} e^{-k^2\lambda^2} \mathcal{F}_H(k). \tag{5.1}$$

they are independent of helicity, and can be constrained through helicity-independent measurements such as the CMB Faraday rotation [22–24].

To constrain magnetic helicity, one has to consider parity odd CMB spectra as outlined in [125, 134, 141]. An upper bound on magnetic helicity can also be obtained via the realizability condition if one can limit independently the amplitude of the magnetic field (i.e., the mean magnetic energy density, $\mathcal{E}_M$) and the correlation length of the field. There are two independent ways of constraining the mean magnetic energy density: (i) the CMB Faraday rotation measurement that is independent of magnetic helicity [24]; (ii) magnetic field effects on the matter power spectrum, i.e., the limitation of the magnetic field amplitude through LSS (in particular Ly-α statistics) [127]. The later gives stronger bounds of the order of nanoGauss. The CMB fluctuations can be expressed in terms of the mean magnetic energy density and the magnetic helicity density. In fact, for maximally helical fields, a combination that determines the strength of the parity-odd signal in the CMB, is $\mathcal{E}_M\mathcal{H}_M$, see equation (18) of Ref. [141]. Thus, the upper bound of this quantity for primordial magnetic fields (independently of the magnetogenesis scenario) is of the order of $10^{-18}\xi_M$ Gauss^2. For a causally generated magnetic field, the correlation length scale must be less than the Hubble horizon at the moment of generation. For cosmological phase transitions, even accounting for hydromagnetic turbulence decay, in the most optimistic scenario, the comoving value of the correlation length is of the order of $30 - 50$ kpc, and thus $\mathcal{E}_M\mathcal{H}_M$ is limited to be less than a few 10^{-20} Gauss^2 Mpc, while the CMB parity odd fluctuations might be sourced if $\mathcal{E}_M\mathcal{H}_M$ is of the order of 10^{-17} Gauss^2 Gpc which is 5–6 orders of magnitude larger than what can be obtained from magnetic fields generated in a phase transition. Therefore, we conclude that if magnetic helicity traces will be detected on the CMB, it will be a direct indication that magnetic helicity has originated in the inflationary epoch.

6 Conclusions

In this paper we have addressed the main statistical properties of helical magnetic fields, applying methods that are well established in the theory of turbulence, mainly following statistical fluid dynamics à la Monin and Yaglom [128] and generalizing it to the helical case. We have also described in detail the different definitions of helicity, such as magnetic, current, and kinetic helicity, and we have made direct connections between them. An important focus has been on the characteristic length scales of the magnetic field such as the correlation and diffusion scales. We have argued that the Alfvén damping scale used in earlier work should be replaced by the proper diffusion length scales of the turbulence where the scale-dependent Reynolds number is unity.

As expected, the energy density of the magnetic field does not depend on the helical part of the correlation function (or the spectrum). Also the rms value of the magnetic energy density is independent of magnetic helicity, even though the four-point correlation function of the magnetic field does contain information on the antisymmetric part (quadratically) [125, 129, 134, 141].

In addition to a theoretical study of the properties of nearly scale-invariant helical magnetic fields and their evolution, we have addressed its cosmological applications. We have shown that, due to the magnetic decay since the moment of generation until recombination, causally generated magnetic field cannot contribute to the CMB fluctuations at currently or near-future observable levels. Firstly, even in the most optimistic situation, the magnetic field strength at generation is limited by the BBN bound being of the order of 10^{-6} Gauss. Secondly, even if the correlation length of the magnetic field is of the order of the Hubble scale at the moment of magnetogenesis and the magnetic field experiences an inverse cascade, the correlation length at recombination is much too small for such fields to leave an imprint on the CMB, see also Fig. 11 of Ref. [124].

At this point *only* a nearly scale invariant spectrum possibly generated during inflation might sustain the amplitude order of $10^{-9} - 10^{-10}$ Gauss with large enough correlation length scale and with substantial magnetic helicity (bounded by the realizability condition) can leave of any traces on CMB maps which are accessible to present and near future observations.

Acknowledgments

A Fourier transform of the magnetic two-point correlation function

We present here the derivation of equation (2.11). The treatment follows [142]. We begin with the two-point correlation function

$$\mathcal{B}_{ij}(\mathbf{r}_1, \mathbf{r}_2) = \langle B_i(\mathbf{r}_1) B_j(\mathbf{r}_2) \rangle. \tag{A.1}$$

To compute its Fourier transform, we first write

$$\mathcal{B}_{ij}(\mathbf{r}_1, \mathbf{r}_2) = \frac{1}{(2\pi)^6} \int d^3\mathbf{k} \int d^3\mathbf{k}' \, \langle B_i^\star(\mathbf{k}) B_j(\mathbf{k}') \rangle e^{-i(\mathbf{k}\cdot\mathbf{r}_1 - \mathbf{k}'\mathbf{r}_2)}. \tag{A.2}$$

Statistical homogeneity implies that $B_{ij}(\mathbf{r}_1, \mathbf{r}_2)$ is a function of $\mathbf{r} = \mathbf{r}_2 - \mathbf{r}_1$ only, so we must have

$$\langle B_i^\star(\mathbf{k}) B_j(\mathbf{k}') \rangle = (2\pi)^3 \delta^{(3)}(\mathbf{k} - \mathbf{k}') \mathcal{F}_{ij}(\mathbf{k}), \tag{A.3}$$

for some function $\mathcal{F}_{ij}(\mathbf{k})$. Then,

$$\mathcal{B}_{ij}(\mathbf{r}) = \frac{1}{(2\pi)^3} \int d^3\mathbf{k} \, e^{-i\mathbf{k}\cdot\mathbf{r}} \mathcal{F}_{ij}(\mathbf{k}). \tag{A.4}$$

B Root-mean-square magnetic energy density

The purpose of this appendix is to present the detailed derivation of equation (2.27). We compute the rms magnetic energy density given as,

$$\mathcal{E}_{\mathrm{M}}^{\mathrm{rms}} = \left(\frac{1}{(2\pi)^3} \int d^3\mathbf{k} \, \mathcal{R}_{\mathrm{M}}(\mathbf{k}) \right)^{1/2}, \tag{B.1}$$

where $\mathcal{R}_{\mathrm{M}}(\mathbf{k})$ is the power spectrum defined through

$$\langle \rho_{\mathrm{M}}^\star(\mathbf{k}) \rho_{\mathrm{M}}(\mathbf{k}') \rangle = (2\pi)^3 \delta^{(3)}(\mathbf{k} - \mathbf{k}') \mathcal{R}_{\mathrm{M}}(\mathbf{k}). \tag{B.2}$$

A short calculation using Wick's theorem gives

$$\mathcal{R}_{\mathrm{M}}(\mathbf{k}) = \frac{\delta^{(3)}(\mathbf{k})}{4(2\pi)^6} \left(\int d^3\mathbf{p} \mathcal{F}_{ii}(\mathbf{p}) \right)^2 + \frac{1}{2(2\pi)^6} \int d^3\mathbf{p} \mathcal{F}_{ij}(\mathbf{p}) \mathcal{F}_{ij}(\mathbf{k} - \mathbf{p}). \tag{B.3}$$

In the next step we use expression (2.14) for $\mathcal{F}_{ij}(\mathbf{k})$. With this we obtain

$$\begin{aligned}
\mathcal{R}_{\mathrm{M}}(\mathbf{k}) = {}& \frac{\delta^{(3)}(\mathbf{k})}{(2\pi)^6} \left(\int d^3\mathbf{p} \mathcal{F}_{\mathrm{N}}(p) \right)^2 \\
& + \frac{1}{(2\pi)^6} \int d^3\mathbf{p} \mathcal{F}_{\mathrm{N}}(p) \mathcal{F}_{\mathrm{N}}(|\mathbf{k} - \mathbf{p}|)(1 + \mu^2) + \frac{4}{(2\pi)^6} \int d^3\mathbf{p} \mathcal{F}_{\mathrm{H}}(p) \mathcal{F}_{\mathrm{H}}(|\mathbf{k} - \mathbf{p}|)\mu,
\end{aligned} \tag{B.4}$$

where $\mu = \hat{\mathbf{p}} \cdot \widehat{(\mathbf{k} - \mathbf{p})}$

To compute the rms of the magnetic field energy density we use Eq. (B.1), and we obtain

$$(\mathcal{E}_\mathrm{M}^\mathrm{rms})^2 = \mathcal{I}_1 + \mathcal{I}_2 + \mathcal{I}_3 \tag{B.5}$$

with

$$\mathcal{I}_1 = \frac{1}{(2\pi)^6} \int d^3\mathbf{k}\, \delta^{(3)}(\mathbf{k}) \left(\int d^3\mathbf{p} \mathcal{F}_{ii}(\mathbf{p}) \right)^2 = \frac{1}{(2\pi)^6} \left(\int d^3\mathbf{p}\, \mathcal{F}_\mathrm{N}(p) \right)^2 , \tag{B.6}$$

$$\mathcal{I}_2 = \frac{1}{(2\pi)^6} \int d^3\mathbf{k} \int d^3\mathbf{p}\, \mathcal{F}_\mathrm{N}(p)\mathcal{F}_\mathrm{N}(|\mathbf{k}-\mathbf{p}|)\,(1+\mu^2)\,, \tag{B.7}$$

$$\mathcal{I}_3 = \frac{4}{(2\pi)^6} \int d^3\mathbf{k} \int d^3\mathbf{p}\, \mathcal{F}_\mathrm{H}(p)\mathcal{F}_\mathrm{H}(|\mathbf{k}-\mathbf{p}|)\,\mu\,. \tag{B.8}$$

To proceed we use the variables transform $\mathbf{q} = \mathbf{k} - \mathbf{p}$, so $d^3\mathbf{q} = d^3\mathbf{k}$.

The integral $\mathcal{I}_1$ is simply

$$\mathcal{I}_1 = \frac{1}{3}\mathcal{E}_\mathrm{M}^2. \tag{B.9}$$

Under the exchange of variables the integral $\mathcal{I}_2$ becomes

$$\mathcal{I}_2 = \int d^3\mathbf{q} \int d^3\mathbf{p}\, \mathcal{F}_\mathrm{N}(p)\mathcal{F}_\mathrm{N}(q) \left[1 + \left(\hat{\mathbf{p}} \cdot \hat{\mathbf{q}} \right)^2 \right]. \tag{B.10}$$

Now, let us write

$$\mu = (\hat{\mathbf{p}} \cdot \hat{\mathbf{q}}) = \frac{4\pi}{3} \sum_{m=-1}^{1} Y_{1m}^\star(\hat{\mathbf{p}}) Y_{1m}^\star(\hat{\mathbf{q}}), \tag{B.11}$$

where $Y_{lm}(\hat{\mathbf{k}})$ are the spherical harmonics. Thus,

$$\mu^2 = \left(\frac{4\pi}{3} \right)^2 \sum_{m=-1}^{1} \sum_{m'=-1}^{1} \left[Y_{1m}^\star(\hat{\mathbf{p}}) Y_{1m'}(\hat{\mathbf{p}}) Y_{1m}(\hat{\mathbf{q}}) Y_{1m'}^\star(\hat{\mathbf{q}}) \right], \tag{B.12}$$

and we use

$$\int_{\Omega_k} d^2\hat{\mathbf{n}}\, Y_{1m}^\star(\hat{\mathbf{k}}) Y_{1m'}(\hat{\mathbf{k}}) = \delta_{mm'}\,, \tag{B.13}$$

so that

$$\int d^2\hat{\mathbf{p}} \int d^2\hat{\mathbf{q}} \left[1 + \left(\hat{\mathbf{p}} \cdot \hat{\mathbf{q}} \right)^2 \right] = (4\pi)^2 \left[1 + \frac{1}{3} \right]\,, \quad \text{and} \quad \mathcal{I}_2 = \frac{4}{3}\mathcal{E}_\mathrm{M}^2. \tag{B.14}$$

Finally, to compute $\mathcal{I}_3$, as above, we use exchange of variables and get, using Eq. (B.11),

$$\mathcal{I}_3 = \frac{4}{(2\pi)^6} \int d^3\mathbf{q} \int d^3\mathbf{p}\, \mathcal{F}_\mathrm{H}(p)\mathcal{F}_\mathrm{H}(q) \sum_{m=-1}^{1} Y_{lm}^\star(\hat{\mathbf{p}}) Y_{lm}(\hat{\mathbf{q}}) = 0, \tag{B.15}$$
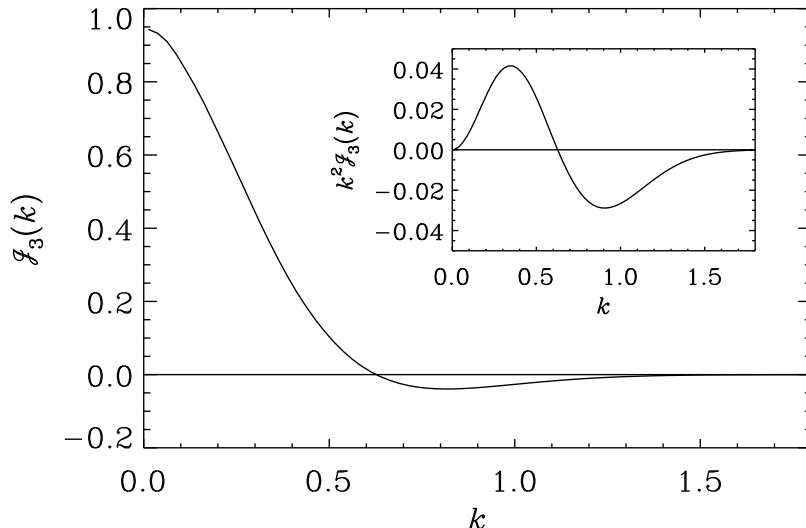
where we have used $\int d^2\hat{\mathbf{n}} Y_{1m}(\hat{\mathbf{n}}) = 0$. Collecting all the terms gives $\mathcal{E}_\mathrm{M}^\mathrm{rms} = \sqrt{\frac{5}{3}}\mathcal{E}_\mathrm{M}$.

We have seen that $\mathcal{I}_3$ given by the double integral over $\mathbf{p}$ and $\mathbf{k}$ vanishes. However, the angular k integral of eq. (B.7) is finite for small k, as seen in the bottom left panel of figure 1 of ref. [129]. This angular integral is defined as

$$\mathcal{J}_3(k) = \int_{-\infty}^{\infty} d^3\boldsymbol{p} \int_{4\pi} k^2 d\Omega_k\, \mathcal{F}_\mathrm{H}(p)\mathcal{F}_\mathrm{H}(q)\, \hat{\boldsymbol{p}} \cdot \hat{\boldsymbol{q}} \tag{B.16}$$

and it satisfies $\mathcal{I}_3 = \frac{4}{(2\pi)^6} \int_0^\infty dk\, k^2\, \mathcal{J}_3(k) = 0$.

Figure 9. Result for $\mathcal{J}_3(k)$. The inset shows $k^2\mathcal{J}_3(k)$. The areas underneath the positive and negative parts are equal, so $\int dk\, k^2\mathcal{J}_3(k) = 0$.

To gain some insight into the functional form of $\mathcal{J}_3(k)$, we adopt as an example a Gaussian for $\mathcal{F}_{\mathrm{H}}(p)$, i.e.,

$$\mathcal{F}_{\mathrm{H}}(p) = \exp(-p^2/2p_0^2), \tag{B.17}$$

with $p_0 = 0.3$ and compute $\mathcal{J}_3(k)$ numerically. The result is shown in figure 9. We see that, although $\int_0^\infty dk\, k^2\mathcal{J}_3(k) = 0$, the integral $\int_0^{k_{\max}} dk\, k^2\mathcal{J}_3(k)$ does not vanish for sufficiently small values of $k_{\max}$.

In the early universe, due to the high conductivity, the Reynolds numbers are very high, and it is reasonably expected that $k_{\max} \gg k_I$,[11] but we see that the integral converges to zero if $k_{\max}/k_I \gtrsim \mathcal{O}(1)$. There might exist some integral measurable quantity determined by the intermediate value k_q, such that $\tilde{\mathcal{I}}_3 = \int_0^{k_q} dk\, k^2\, \mathcal{J}_3(k)$ is nonvanishing. In such a case, care must be taken to interpret those quantities, since the dependence on helicity in that case could be affected by measurement details. The sign of magnetic helicity, however, cannot enter such a dependence.

References

[1] L. M. Widrow, Rev. Mod. Phys. **74**, 775 (2002).

[2] R. Durrer and A. Neronov, Astron. Astrophys. Rev. **21**, 62 (2013).

[3] K. Subramanian, Rept. Prog. Phys. **79**, 076901 (2016).

[4] J. P. Vallée, New Astron. Rev. **48**, 763 (2004).

[5] M. L. Bernet, F. Miniati, S. J. Lilly, P. P. Kronberg and M. Dessauges-Zavadsky, Nature **454**, 302 (2008).

[6] P. P. Kronberg, M. L. Bernet, F. Miniati, S. J. Lilly, M. B. Short and D. M. Higdon, Astrophys. J. **676**, 7079 (2008).

[7] R. M. Kulsrud and E. G. Zweibel, Rept. Prog. Phys. **71**, 0046091 (2008).

[8] A. Kandus, K. E. Kunze and C. G. Tsagas, Phys. Rept. **505**, 1 (2011).

[9] A. Neronov and I. Vovk, Science **328**, 73 (2010).

[10] F. Tavecchio, G. Ghisellini, G. Bonnoli and L. Foschini, Mon. Not. Roy. Astron. Soc. **414**, 3566 (2011).

---

[11] For Kolmogorov spectra, the Reynolds number is given by $\mathrm{Re} = (k_D/k_I)^{4/3}$ thus $k_D \gg k_I$,

[11] W. Essey, S. Ando and A. Kusenko, Astropart. Phys. **35**, 135 (2011).

[12] A. M. Taylor, I. Vovk and A. Neronov, Astron. Astrophys. **529**, A144 (2011).

[13] H. Huan, T. Weisgarber, T. Arlen and S. P. Wakely, Astrophys. J. **735**, L28 (2011).

[14] I. Vovk, A. M. Taylor, D. Semikoz and A. Neronov, Astrophys. J. **747**, L14 (2012).

[15] K. Dolag, M. Kachelriess, S. Ostapchenko and R. Tomas, Astrophys. J. **727**, L4 (2011).

[16] C. D. Dermer, M. Cavadini, S. Razzaque, J. D. Finke and B. Lott, Astrophys. J. **733**, L21 (2011).

[17] K. Takahashi, M. Mori, K. Ichiki and S. Inoue, Astrophys. J. **744**, L7 (2012).

[18] J. D. Finke, L. C. Reyes, M. Georganopoulos, K. Reynolds, M. Ajello, S. J. Fegan and K. McCann, Astrophys. J. **814**, 20 (2015).

[19] T. C. Arlen, V. V. Vassiliev, T. Weisgarber, S. P. Wakely and S. Y. Shafi, Astrophys. J. **796**, 18 (2014).

[20] C. Tsagas and R. Maartens, Phys. Rev. D **61**, 083519 (2000).

[21] P. A. R. Ade et al. [POLARBEAR Collaboration], Phys. Rev. D **92**, 123509 (2015).

[22] T. Kahniashvili, New Astron. Rev. **49**, 79 (2005).

[23] L. Campanelli, A. D. Dolgov, M. Giannotti and F. L. Villante, Astrophys. J. **616**, 1 (2004).

[24] A. Kosowsky, T. Kahniashvili, G. Lavrelashvili and B. Ratra, Phys. Rev. D **71**, 043006 (2005).

[25] P. P. Kronberg, M. Simard-Normandin, Nature, **263**, 653 (1976).

[26] P. P. Kronberg, J. J. Perry, Astrophys. J. **263**, 518 (1982).

[27] P. Blasi, S. Burles, A. V. Olinto Astrophys. J. **514**, L79, (1999).

[28] E. Komatsu, et al. [WMAP Collaboration], Astrophys. J. Suppl. **180**, 330 (2009).

[29] D. G. Yamazaki and M. Kusakabe, Phys. Rev. D **86**, 123006 (2012).

[30] P. A. R. Ade et al. [Planck Collaboration], Astron. Astrophys. **594**, A19 (2016).

[31] F. Miniati and A. R. Bell, "Resistive Magnetic Field Generation at Cosmic Dawn," Astrophys. J. **729**, 73 (2011).

[32] M. S. Turner and L. M. Widrow, Phys. Rev. D **37**, 2743 (1988).

[33] B. Ratra, Astrophys. J. **391**, L1 (1992).

[34] K. Bamba and J. Yokoyama, Phys. Rev. D **69**, 043507 (2004).

[35] K. Atmjeet, I. Pahwa, T.R. Seshadri, and K. Subramanian Phys. Rev. D **89**, 063002 (2104).

[36] A. D. Dolgov, Phys. Rev. D, **48**, 2499, (1993).

[37] D. Lemoine and M. Lemoine, Phys. Rev. D **52**, 1955 (1995).

[38] M. Gasperini, M. Giovannini and G. Veneziano, Phys. Rev. Lett. **75**, 3796 (1995).

[39] J. Martin and J. Yokoyama, JCAP **0801**, 025 (2008).

[40] G. Lambiase, S. Mohanty and G. Scarpetta, JCAP **0807**, 019 (2008).

[41] L. Campanelli, Int. J. Mod. Phys. D **18**, 1395 (2009).

[42] L. Campanelli, P. Cea, G. L. Fogli and L. Tedesco, Phys. Rev. D **77**, 043001 (2008).

[43] L. Campanelli and P. Cea, Phys. Lett. B **675**, 155 (2009).

[44] K. E. Kunze, Phys. Rev. D **81**, 043526 (2010).

[45] J. Beltran Jimenez and A. L. Maroto, Phys. Rev. D **83**, 023514 (2011).

[46] R. Durrer, L. Hollenstein and R. K. Jain, JCAP **1103**, 037 (2011).

[47] M. Das and S. Mohanty, Int. J. Mod. Phys. A **27**, 1250040 (2012).

[48] F. A. Membiela and M. Bellini, JCAP **1010**, 001 (2010).

[49] K. Bamba, C. Q. Geng, S. H. Ho and W. F. Kao, Eur. Phys. J. C **72**, 1978 (2012).

[50] R. K. Jain, R. Durrer and L. Hollenstein, J. Phys. Conf. Ser. **484**, 012062 (2014).

[51] K. Bamba, C. Q. Geng and L. W. Luo, JCAP **1210**, 058 (2012).

[52] J. B. Jimenez and A. L. Maroto, Springer Proc. Phys. **137**, 215 (2011).

[53] C. T. Byrnes, L. Hollenstein, R. K. Jain and F. R. Urban, JCAP **1203**, 009 (2012).

[54] R. R. Caldwell, L. Motta and M. Kamionkowski, Phys. Rev. D **84**, 123525 (2011).

[55] C. Bonvin, C. Caprini and R. Durrer, Phys. Rev. D **86**, 023519 (2012).

[56] F. A. Membiela and M. Bellini, Eur. Phys. J. C **72**, 2181 (2012).

[57] T. Fujita and S. Mukohyama, JCAP **1210**, 034 (2012).

[58] L. Motta and R. R. Caldwell, Phys. Rev. D **85**, 103532 (2012).

[59] L. Campanelli, Phys. Rev. Lett. **111**, 061301 (2013).

[60] T. Fujita, R. Namba, Y. Tada, N. Takeda and H. Tashiro, JCAP 2015 054 (2015).

[61] L. Sorbo, JCAP 06 003 (2011).

[62] C. Caprini and L. Sorbo, JCAP 056 (2014).

[63] P. Adshead, J. T. Giblin, T. R. Scully and E. I. Sfakianakis, JCAP **1512**, 034 (2015).

[64] P. Adshead, J. T. Giblin, T. R. Scully and E. I. Sfakianakis, JCAP **1610**, 039 (2016).

[65] V. Demozzi, V. Mukhanov and H. Rubinstein, JCAP **0908**, 025 (2009).

[66] S. Kanno, J. Soda and M. a. Watanabe, JCAP **0912**, 009 (2009).

[67] F. R. Urban, JCAP **1112**, 012 (2011).

[68] V. Demozzi and C. Ringeval, JCAP **1205**, 009 (2012).

[69] R. Sharma, S. Jagannathan, T. R. Seshadri and K. Subramanian, Phys. Rev. D **96**, 083511 (2017).

[70] R. Sharma, K. Subramanian and T. R. Seshadri, arXiv:1802.04847 [astro-ph.CO].

[71] G. Tasinato, JCAP **1503**, 040 (2015).

[72] L. Campanelli, Eur. Phys. J. C **75**, 278 (2015).

[73] R. J. Z. Ferreira, R. K. Jain and M. S. Sloth, JCAP **1310**, 004 (2013)

[74] R. J. Z. Ferreira, R. K. Jain and M. S. Sloth, JCAP **1406**, 053 (2014)

[75] E. R. Harrison, Mon. R. Astron. Soc. **147**, 279 (1970).

[76] J. M. Quashnock, A. Loeb and D. N. Spergel, Astrophys. J. **344**, L49 (1989).

[77] T. Vachaspati, Phys. Lett. B **265**, 258 (1991).

[78] J. M. Cornwall, Phys. Rev. **D 56**, 6146, (1997).

[79] M. Giovannini and M. E. Shaposhnikov, Phys. Rev. D **57**, 2186 (1998).

[80] G. Sigl, A. V. Olinto and K. Jedamzik, Phys. Rev. D **55**, 4582 (1997).

[81] M. Joyce and M. E. Shaposhnikov, Phys. Rev. Lett. **79**, 1193 (1997).

[82] G. B. Field and S. M. Carroll, Phys. Rev. D **62**, 103008 (2000).

[83] M. Hindmarsh and A. Everett, Phys. Rev. D **58**, 103505 (1998).

[84] K. Enqvist, Int. J. Mod. Phys. **D 7**, 331 (1998).

[85] D. Grasso and A. Riotto, Phys. Lett. B **418**, 258 (1998).

[86] J. Ahonen and K. Enqvist, Phys. Rev. **D 57**, 664 (1998).

[87] M. Giovannini, Phys. Rev. **D 61**, 063004 (2000).

[88] T. Vachaspati, Phys. Rev. Lett. **87**, 251302 (2001).

[89] A. D. Dolgov and D. Grasso, Phys. Rev. Lett. **88**, 011301 (2002).

[90] G. Sigl, Phys. Rev. D **66**, 123002 (2002).

[91] D. Grasso and A. Dolgov, Nucl. Phys. Proc. Suppl. **110**, 189 (2002).

[92] D. Boyanovsky, H. J.de Vega, and M. Simionato, Phys. Rev. **D 67**, 023502 (2003).

[93] D. Boyanovsky, H. J. de Vega and M. Simionato, Phys. Rev. **D 67**, 123505 (2003).

[94] V. B. Semikoz and D. D. Sokoloff, Astron. Astrophys. **433**, L53 (2005);

[95] V. B. Semikoz and D. D. Sokoloff, Int. J. Mod. Phys. D **14**, 1839 (2005).

[96] A. Diaz-Gil, J. Garcia-Bellido, M. Garcia Perez, and A. Gonzalez-Arroyo, Phys. Rev. Lett. **100**, 241301 (2008).

[97] T. Stevens, M. B. Johnson, L. S. Kisslinger, E. M. Henley, W.-Y. P. Hwang, and M. Burkardt, Phys. Rev. **D 77**, 023501 (2008).

[98] E. M. Henley, M. B. Johnson, and L. S. Kisslinger, Phys. Rev. D **81**, 085035 (2010).

[99] F. R. Urban and A. R. Zhitnitsky, Phys. Rev. D **82**, 043524 (2010).

[100] T. Stevens, M. B. Johnson, L. S. Kisslinger and E. M. Henley, Phys. Rev. D **85**, 063003 (2012).

[101] A. Boyarsky, J. Frohlich and O. Ruchayskiy, Phys. Rev. Lett., **108**, 031301 (2012).

[102] R. Durrer and C. Caprini, JCAP **0311**, 010 (2003)

[103] E. Witten, Phys. Rev. D **30**, 272 (1984).

[104] C. J. Hogan, Phys. Rev. Lett. **51**, 1488 (1983).

[105] D. Boyanovsky, H. J. de Vega, and D. J. Schwarz, Ann.Rev.Nucl.Part.Sci. **56:441-500**, (2006).

[106] Y. Aoki, G. Endrodi, Z. Fodor, S. D. Katz and K. K. Szabo, Nature **443**, 675 (2006)

[107] Kajantie, K. and Laine, M. and Rummukainen, K. and Shaposhnikov, M., Phys. Rev. Lett. **77**, 2887 (1996).

[108] F. Csikor, Z. Fodor and J. Heitger, Nuclear Physics B (Proc. Suppl.) 63 A-C (1998).

[109] D. J. Schwarz and M. Stuke JCAP **0911**, 025 (2009).

[110] D. S. Gorbunov and V. A. Rubakov Singapore: World Scientific (2011)

[111] K. Subramanian and A. Brandenburg, Phys. Rev. Lett. **93**, 205001 (2004).

[112] L. Campanelli and M. Giannotti, Phys. Rev. D **72**, 123001 (2005).

[113] H. Tashiro, T. Vachaspati and A. Vilenkin, Phys. Rev. D **86**, 105033 (2012).

[114] L. Sriramkumar, K. Atmjeet and R. K. Jain, JCAP **1509**, 010 (2015).

[115] T. Kahniashvili, A. G. Tevzadze, A. Brandenburg and A. Neronov, Phys. Rev. D **87**, 083007 (2013).

[116] C. J. Copi, F. Ferrer, T. Vachaspati, and A. Achúcarro Phys. Rev. Lett. **101** 171302 (2008).

[117] A. Brandenburg, T. Kahniashvili and A. G. Tevzadze, Phys. Rev. Lett. **114**, 075001 (2015).

[118] T. Kahniashvili, A. Brandenburg, R. Durrer, A. G. Tevzadze and W. Yin, JCAP **1712**, 002 (2017).

[119] H. K. Moffatt 1978, *Magnetic Field Generation in Electrically Conducting Fluids* (Cambridge: Cambridge Univ. Press)

[120] A. Brandenburg and T. Kahniashvili, Phys. Rev. Lett. **118**, 055102 (2017).

[121] A. Brandenburg, K. Enqvist and P. Olesen, Phys. Rev. D **54**, 1291 (1996).

[122] A. Brandenburg and W. Dobler, Comput. Phys. Commun. **147**, 471 (2002).

[123] F. Vazza, M. Brüggen, C. Gheller, S. Hackstein, D. Wittor and P. M. Hinz, Class. Quant. Grav. **34**, no. 23, 234001 (2017)

[124] A. Brandenburg, T. Kahniashvili, S. Mandal, A. R. Pol, A. G. Tevzadze and T. Vachaspati, Phys. Rev. D **96**, 123528 (2017).

[125] C. Caprini, R. Durrer and T. Kahniashvili, Phys. Rev. D **69** 063006 (2004).

[126] T. Kahniashvili and B. Ratra, Phys. Rev. D **71**, 103006 (2005).

[127] T. Kahniashvili, Y. Maravin, A. Natarajan, N. Battaglia and A. G. Tevzadze, Astrophys. J. **770**, 47 (2013).

[128] A. S. Monin and A. M. Yaglom. *Statistical Fluid mechanics mechanics of turbulence*, vol. 2. MIT press, Cambridge, 1971.

[129] M. Ballardini, F. Finelli and D. Paoletti, JCAP **1510**, 031 (2015)

[130] K. Dolag, M. Bartelmann, and H. Lesch, Astron. Astrophys. **348**, 351 (1999)

[131] K. Dolag, M. Bartelmann, and H. Lesch, Astron. Astrophys. **387**, 383 (2002).

[132] V. I. Arnold, B. A. Khesin, Ann. Rev. Fluid Dyn. **24**, 145 (1992).

[133] M. A. Berger, Plasma Physics and Controlled Fusion **41** 167 (1999).

[134] K. E. Kunze, Phys. Rev. D **85**, 083004 (2012).

[135] K. Subramanian and A. Brandenburg, Astrophys. J. **648**, L71 (2006).

[136] V. I. Arnold, "*The asymptotic Hopf invariant and its applications*" from "Vladimir I. Arnold - Collected Works: Hydrodynamics, Bifurcation Theory, and Algebraic Geometry 1965-1972", Springer Berlin Heidelberg, 2014.

[137] A. Brandenburg and K. Subramanian, Phys. Rept. **417**, 1 (2005).

[138] S. Sur, A. Brandenburg, and K. Subramanian, Mon. Not. Roy. Astron. Soc. **385**, L15 (2008).

[139] T. Kahniashvili, A. G. Tevzadze, S. K. Sethi, K. Pandey and B. Ratra, Phys. Rev. D **82**, 083005 (2010)

[140] A. Zucca, Y. Li and L. Pogosian, Phys. Rev. D **95**, no. 6, 063506 (2017)

[141] T. Kahniashvili, Y. Maravin, G. Lavrelashvili and A. Kosowsky, Phys. Rev. D **90** 083004 (2014).

[142] L. D. Landau and E. M. Lifshitz, *Fluid Mechanics*, 1982